BILINGUAL PUBLISHING CO.
Pioneer of Global Academics Since 1984

Journal of Atmospheric Science Research

Volume 4 • Issue 4 • October 2021 ISSN 2630-5119(Online)

BILINGUAL PUBLISHING CO.
Pioneer of Global Academics Since 1984

Volume 4 Issue 4 • October 2021 • ISSN 2630-5119 (Online)

Journal of Atmospheric Science Research

BILINGUAL PUBLISHING CO.

Pioneer of Global Academics Since 1984

BILINGUAL PUBLISHING CO.
Pioneer of Global Academics Since 1984

Volume 4 | Issue 4 | October 2021 | Page1-49
Journal of Atmospheric Science Research

Contents

Articles

Review

BILINGUAL PUBLISHING CO.
Pioneer of Global Academics Since 1984

Journal of Atmospheric Science Research
https://ojs.bilpublishing.com/index.php/jasr

REVIEW

Low Adaptive Capacity in Africa and Climate Change Crises

Victor Adjei[1*] Elijah Foh Amaning[2]

1. Climate Change and Sustainable Development, University of Ghana, Legon, Ghana
2. Environmental Science, University of Ghana, Legon, Ghana

ARTICLE INFO

Article history
Received: 16 September 2021
Accepted: 12 October 2021
Published: 21 October 2021

Keywords:
Food security
Variability
Methane
Atmosphere
Conflict

ABSTRACT

The changing climate is unequivocal, and it is generally recognised as a threat to the terrestrial environment due to its cross-sectoral and irreversible impacts. Since the inception of industrial revolution (1750), the concentration of greenhouse gases (carbon dioxide, methane and nitrous oxide) in the atmosphere has been compromised. Until the past two centuries, the quantity of carbon dioxide and methane in the atmosphere had never surpassed about 280 part per million (ppm) and 790 part per billion (ppb), respectively. Rise in greenhouse gases (GHGs) has impacted almost every biotic component on the surface of the earth, and regions which have low adaptive capacity and greatly depend on agriculture and biodiversity for livelihood are hard hit. This phenomenon has resulted in global warming, extinction of some fora and fauna species, precipitation variability, extreme weather conditions, migration of biotic creatures from one geographical area to another, melting of icecap, sea level rise, coral breach and so on during the last century.

The contribution of emission of greenhouse gases of Africa is insignificant, however, the repercussion of the changing climate is crucial in the region due to the presence of other stressors such as poverty, corruption, diseases, geographical position of the continent, low adaptive capacity, rain-fed agriculture etc., and this has led to conflict over resources usage, food insecurity, forced migration, ill-health and many more.

1. Introduction

One of the greatest challenges giving headache to the entire globe is the changing climate. It is projected that [1], 50 years to come, global warming will exacerbate to the detriment of humanity. Extremities of weather conditions such as cyclones, tsunami, droughts, flooding etc. will take place more frequently and forcefully, triggering insecure livelihood conditions, shortage of food, forced migration, water inadequacy and conflict.

It is worthy to note that anthropogenic climate change is already altering weather trends and worsening conditions of weather. Previously, short-term conditions namely droughts, cyclones and flooding are currently longer, more regular and intensified with long-felt socio-economic impacts [1].

The Secretary General of United Nations, in March, 2018, christened climate change as 'the most systemic threat to humankind' [2]. Anthropogenic activities have warmed the lower atmosphere (troposphere) by approximately 1°C above the pre-industrial level, and it is really causing havoc to the survival of living creatures. Carbon

*Corresponding Author:
Victor Adjei,
Climate Change and Sustainable Development, University of Ghana, Legon, Ghana;
Email: victoradjei73@gmail.com

DOI: https://doi.org/10.30564/jasr.v4i4.3723

dioxide (CO_2), which is the major component of greenhouse gases (GHGs) accountable for the continuous warming of the earth atmosphere, was incomparable in some million years ago [3]. Humankind has emitted CO_2 14,000 times faster than nature itself has, over the past 600,000 years, released [4]. In effect, the social environment and physical system of earth are experiencing fundamental alteration of which many are irrevocable [5].

According to records [6], the three decades have realised consecutively warmer air temperatures than any other since 1850. Both troposphere and oceans are heating up, icecap are incessantly melting and sea level is rising, and it (sea) is more acidic than it has been for the last 300 million years [3]. Normal trend in climate is fast disappearing. Globally, the negative repercussion of changing climate is felt by all biotic phenomena and natural catastrophes have become almost permanent.

It is believed that global warming would persist and changing climate impacts will get worse over the near future as a result of past emission inertia in the climate system [7]. However, scale of effects beyond 2050, relies on the degree of which GHGs emissions are collectively and immediately reduced. Failure of the world leaders to cut emission of GHGs, warming of 4°C above the pre-industrial level would occur by 2100 [3]. As a matter of fact, in a world of 4°C, the threshold for adaptation of humankind are likely to be superseded in several regions globally, whereas the limits for natural system adaptation will greatly be surpassed worldwide [8].

2. Climate of Africa: Past and Present

It is perceptible that mean atmospheric temperatures have become warmer than usual over the surface of the Earth. According to National Oceanic Atmospheric Administration [9], these changes became explicit in Africa beginning in somewhere 1975. Since then temperatures within lower atmosphere have risen at a constant rate of approximately 0.03°C annually. As it has been recorded in some parts of Africa where data is available, considerable number of them have on records that extreme temperatures are on the rise including prolong heat waves [10]. Repeatedly, climatic records are being broken all the time. In sub-Saharan Africa, 19 of the past 20 years have realised warmer than any earlier year on record. The current atmospheric temperatures are really hotter than ever felt in the past record. Historic rainfall trends indicate that sub-Saharan Africa is persistently drying up [11]. Western and Southern parts of Africa, notably Zambia and Zimbabwe show swift and statistically substantial fall in rainfall. Research has it that rainfall in the transitional ecological zone of Ghana (middle belt) is characterised by intermittent rainfall coupled with merging of major (March – July) and minor (September and October) seasons [12,13]. The paper further argued that there had been late commencement of major season and early cessation of minor season.

However, Southern Africa, some regions of East and North Africa have witnessed a rise in precipitation. In the same vein, rise in air temperatures leading to higher rates of evapotranspiration, which result in drier soil conditions [14] have been reported. It is on record that between 2001 and 2017, Zambia has experienced constant rise in evaporative stress. Amidst rising rainfall, there is possibility of occurrence of soil aridity. From 1961 to 2000, a rise in incidence of dry spells was occasioned by an increase in the intensification of daily precipitation in southern Africa which impacts on runoff [15].

Undoubtedly, the most susceptible regions and societies to the changing climate repercussions according to the various assessment made are found in sub Saharan Africa [1]. With regards to last century, an increase in global atmospheric temperatures of about 1°C was estimated on the continent of Africa, greater than the terrestrial average. Unambiguously, warming up of the entire globe is occurring with negative effects felt disproportionately. It is sad to note that Africa is particularly defenceless to insignificant changes in precipitation and temperature as its inhabitants could probably adjust to only minor range of climate changeability. The Intergovernmental Panel on Climate Change (IPCC) has recognised ecological and environmental elements that are particularly susceptible to changing climate and to an increase in general temperatures, as most of them are found on African continent [1].

One geographical area of which the changing climate has hard hit is the Horn of Africa, where severe drought as a result of scanty rainfall eventually caused hunger in the year 2011 [1]. It is difficult to prove if it was caused by climate change however, IPCC, scientists and international bodies in the region argue that conditions in weather in the sub-region consistently are being characterised with irregular precipitation and life-threatening events. Whereas IPCC projections forestall wetter climatic conditions for the region, current studies anticipate the contrary and otherwise could occur to be the case, as the area has gone through both intense droughts and flooding in the contemporary past [16].

3. Future Anticipated Climate Model for Africa

General Circulation Models (GMCs) offer the most up-front and scientifically recognised way of projecting future conditions of climate. Nevertheless, the only possible simulations of climate change carried out with GCMs

are at course resolutions (typically 50-100km grid cells) that are not detailed enough to evaluate regional and national effects. The Coupled Model Inter-comparison Project Phase 5 (CMIPS5), which is known to be the current GCMs available, suggests that air temperatures increase for Africa with contemporary emission pathway is 1.7°C by the 2030s, 2.7°C by the 2050s, and 4.5°C by the 2080s. Even under the lowest GHGs emission scenario, climate average, by 2030, is anticipated to be generally different from what has been witnessed historically [17]. What is difficult to project perfectly is future rainfall [18,19].

Again, by 2050, the median CMIPS models state under the higher emission scenario (RCP 80.5) that much of eastern and central Africa would experience rise in annual rainfall whereas reduction would characterised other regions of the continent such as southern, western and northern. It is projected that there will be an increase of precipitation of more than 200mm and over 25 percent yearly are noticed in some regions, as well as decreases of over 100mm and over 20 percent in other areas. As a matter of fact, not all climate models subscribe on the amount or even direction of variation [17]. However, according to Niang *et al.* [20], there are some areas with significant harmony with regards to climate models: more than 80% of the climate models are in agreement with reduction in precipitation in future projection for some regions of northern and southern Africa.

According to Vizy and Cook [21], north-western Sahara of North Africa experienced 40 wave days per year during the 1989-2009 time scale. There is a projected rise in heat wave with regards to number of days over the 21st century [22]. Based on CMIP3, GCMs projection over West Africa, there is low to medium confidence changes of heavy precipitation by the end of the 21st century [10]. Regional model studies estimate rise in the number of extreme precipitation days over western part of Africa including the Sahel during the months of May and July [21] however, the inverse is true in the Guinea Highlands and Cameroun mountains as the region would experience more intense and regular events of rainfall extremities [23,24].

4. Anticipated Changes in Temperature for African Sub-region

Estimated warming is somewhat less robust than that of the global land region which is overall characteristic of the Southern Hemisphere. With regards to the low-emission scenario RCP 2.6 (representing a 2°C world), the summer air temperatures of Africa rises until 2050 at approximately 1.5°C beyond the 1951 – 1980 baseline and be kept steadily at the same rate until the end of the century [25]. With respect to the high-emission scenario of RCP8.5 (representing a 4°C world), terrestrial warming on the African continent persists till the end of the century, with an expected 5°C monthly summer atmospheric temperatures above the 1951 – 1980 baseline by 2100. As a matter of fact, this warming is evenly distributed geographically, even though regions of inland in the sub-tropics warm the fastest. It is projected that under a low-emission scenario (RCP 2.6), only few areas in western tropical Africa will experience significant normalised warming of up to somewhere four standard variations [25].

5. Expected Changes in Precipitation for African Sub-region

With regards to low-emission scenario, the precipitation models are not in agreement with direction of change over vast regions. However, the percentage change, under the high-emission climate models, becomes larger everywhere. The model, because of this stronger signal, disagrees between places getting wetter and regions getting drier. The projection is limited to south-eastern areas and some places in the tropical western Africa for some months such as June, July and August, and to the south-eastern areas for the months of December, January, and February [25]. There is an anticipation of wetting of the Horn of Africa which is part of rainfall extremities captured by the full Coupled Model Inter-comparison Project Phase 5 model ensemble [18]. The paper [18] again made an estimated changes of 5 to 15% comprehensive wet-day rainfall for West African sub-region with a lot of doubts, particularly with regards to monsoon dependent coast of Guinea. Appreciable wet events are projected to occur by 50-100% in eastern tropical Africa and by 30-70 percent in the westerns part of tropical Africa. Again, precipitation for southern Africa suggests that the entire wet-day rainfall forecasted to reduce by percentage between 15-45 (15-45%) and appreciable wet events of rainfall to rise by approximately 20-30 percent over some places of the sub-region. Nevertheless, some localised areas stretching along the coastal belt of southern Africa are anticipated to experience reduction in wet days rising to about 30%. Furthermore, it is on records that persistent rise in dry days with reduction in heavy rainfall showing an intense dry conditions in the region is imminent [18].

Rainfall is forecasted to experience a significant change in different months with regards to its arrival, duration and cessation of the cropping season. For instance, in Tanzania, rainfall is estimated to rise appreciably during rainy season (November-May) and reduce somewhere in the wet season's commencement (September-October) and end in May – June [17]. Generally, rainfall is anticipated to augment, however, the change would be a short-

lived showing both reduction of wet season and ample of rainfall extremities. According to the study, even places witnessing a rise in rainfall regime, there is a probability that worsening water stress would impact crop system negatively neutralising the gains achieved [17]. The amount of the temperature increase, and the changes in cloud cover, depending on timing of rainfall, larger areas are likely to experience water availability both in streams and in the soil, but high air temperatures, however, would lead to water loss in the soil through vegetation in the process of evaporation [14]. Atmospheric temperatures and rainfall alteration have significant repercussion on food system and security on the African sub-region [26,27]. It is quite interesting that rainfall suitability of several food crops is estimated to shift as the warming of the lower atmosphere continues unabated [28]. According to Ramirez-Villegas and Thornton [29], some identified food crops such as maize and beans are expected to experience stern reduction in suitability in several regions on the continent. Persistent rise in the concentration of CO_2 is likely to impact on the content of plants' nutrients leading to substantial disruption of protein and micro-nutrient of these plants in some places in SSA [30,31].

6. Climate Change and Poverty on African Continent

The negative effects of the changing climate and variability strike the poor the hardest due to their low adaptive capacity and exposure. Majority of the populace of sub-Sahara Africa derive their livelihood from natural resources and rain-fed agriculture, and they are unable to adjust well with the attendant ills of anthropogenic climate change such as droughts, flooding, soil erosion and other natural catastrophes [32]. Citizens are entangled in the web of poverty therefore, they would find it extremely difficult to disentangle themselves if changing climate and variability continues to soar. Others who have escaped this episode can also slip back into poverty if people do not see any change with their fragile adaptive capacity. For instance, according to the report of [32], in East Africa, pastoralists who planned to embark on a migration to increase their chance of survival of their animals and themselves from drought-prone environment witnessed livestock diseases, conflict for piece of land for grazing and other such conditions that were likely to push them back into poverty.

Research has it that majority of the population in African sub-region are very poor and the number surpasses 490 million according to World Bank definition of extreme poverty as earning less than US$1.90 per day [7]. Basically, people who have low adaptive capacity to mitigate the ramifications of anthropogenic climate-related crises become extremely vulnerable. The United Nations and other intergovernmental organisations are alarmingly whistling the danger on the extent climate change can compromise strategies meant to curtail poverty. The IPCC has emphatically stated that changing climate would aggravate and further concretise poverty [21] and per World Bank calculation, geophysical and climate-related disasters put an extra 26 million population into poverty worldwide annually [35].

Africa's extremely poor population is estimated to increase for another third time, peaking at 590 million by 2040, before dropping to about 390 million by 2063. These projections ignore those who are likely to slip back into poverty as a result of natural calamities, increasing air temperatures and conflict [7]. This huge number of people in poverty is found in the African sub-region. East and West Africa are the region of the myriad of this large population stricken by extreme poverty. Their combined extremely poor populations (projected 310 million people in 2018) are more than double the number of extremely poor people in the rest of the continent (an estimated of 150 million people in 2018) [7].

7. Agriculture and Food Security

Agriculture offers a source of livelihood to approximately three-quarters of people in the sub-region (SSA), but the sector is predominantly rain-fed. Some phenomena such as flooding, severe and persistent droughts, loss of fertile lands due to desertification, salinisation and soil erosion etc. are decreasing productivity of agricultural produce, but augmenting crop disappointment, loss of livestock to rural populace etc. According to the report of Centre for International Governance Innovation [34], the Horn of Africa's pastoralist region around Ethiopia-Kenya-Somalia border has been sternly hit by recurrent droughts; livestock losses have plunged approximately 11 million people dependent on livestock of their livelihoods into a crisis and generated mass movement of pastoralists out of drought-stricken regions. Again, Northern Africa would not be spared either per the various projections made. The region is already food import-dependent to feed its teeming populace and most agriculture is rain-fed as this characterises the entire Africa. Projected decline in rainfall and rise in average atmospheric temperatures will decrease agricultural production and threaten source of livelihoods of citizens. A study has it that Tunisia, for instance, can anticipate 10-50% reduction in wheat production at 2^{o}C of warming [36]. With regards to Western Africa, studies have shown that transitional ecological zone of Ghana has been battling with incessant erratic rainfall and this has affected maize production especially during the minor season (September- October) [37]. This, according to

the study, has emerged as the cropping system of farmers is mainly rain-fed, and this has pushed majority of the local farmers into cashew production [37,38].

Changing climate is contributing to oceanic acidification and a rise in surface water temperatures across the continent of Africa, inversely impacting on fish stocks and threatening the livelihood of coastal and small-scale fishing communities. The repercussions of climate change and variability on agriculture and other key economic sectors in the food crop production and supply chain such as forestry and energy, threaten food security across the region [39].

According to Food and Agriculture Organisation [37], approximately 923 million citizens are chronically hungry worldwide. The Millennium Development Goals (MDGs) of reducing the malnourished population by half by 2015 became extremely challenging to realise. The food security situation in Africa is very worrying. Approximately, 36 countries globally are facing food insecurity in recent times, 21 of these countries are found in Africa according to the report of [40]. The paper further stated that over 300 million people in Africa are chronically hungry, almost one-third of the population of the region. Out of this figure (300 million), at least, 235 million are in SSA [39] making it the geographical area on the globe with the topmost percentage of chronically hungry persons. The poorest category is the hardest hit on the continent, and this group comprises the landless, female-headed households and urban poor [39]. In addition, most rural and urban households on the African continent depend on food purchases and are likely to lose from exorbitant food prices as they become more susceptible. Real income is reduced by high food prices on the market and this would trigger an increase in the occurrence of food insecurity and undernourishment among the vulnerable who are mostly the poor, marginalised and landless.

According to CIGI [34], the food insecurity in Africa was aggravated by the global financial crunch. Nonetheless, food insecurity remains headache to the leaders of the continent. Prices of basic foodstuffs remain high, and the structural dynamics that supported the crisis are yet to be dealt with. The 2008 crisis according to the paper [34], nevertheless, was a wake-up call for the leaders of Africa. The leaders of the region including her donors need to realise the urgency of solving problems with food crisis as climate change has come to dwell with humankind.

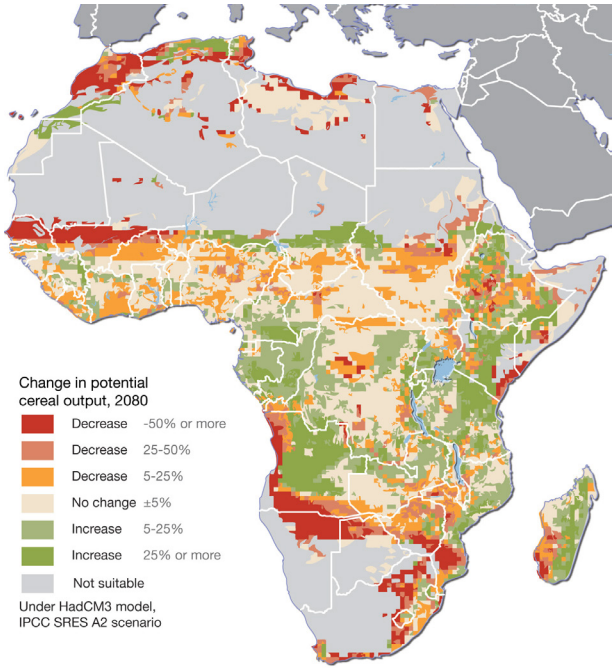

Figure 1. Projected changes in cereal productivity in Africa as a result of climate change – current climate to 2080
Source: Fischer et al. (2005)

The above figure shows clearly the cereal crops are not spared either by climate change and variability. The most affected region is indicated by red up to green colour.

8. Health Challenges

It is undisputable that changing climate is seldom, but tends to be facilitated by already contextual factors to generate effects for human existence [5]. Climate change impacts on human health and facilities,and causes unspeakable injuries due to weather extremity occurrences such as landslides or floods as a result of heavy downpour [41,42]. According to Welborn [7], historic flooding in Nigeria in 2012 took the lives of about 400 people and displaced another 2 million citizens. Flooding in Nigeria has since led to hundreds of deaths and caused for evacuation of hundreds of thousands of people, with almost 200 being put to death by flooding just in a single year (2018).

Extreme heat events can equally lead to heat cramps, collapsing, heat exhaustion, heat stroke, and death, and compromise outdoor events [43]. A study by Azongo *et al.* [44] has it that there are correlations being identified between high atmospheric temperatures and increased all-cause mortality in Ghana and Kenya, with children and the elderly being vulnerable. For instance, cerebrospinal meningitis (CSM) has been reported to be rampant in some parts of Ghana mostly in the northern belt (Sudan Savanna) where the environmental temperature is occasionally high

during dry seasons (November to April) [45]. Drought and flooding conditions affect availability and quality of water leading to illness such as diarrhoea, scabies, trachoma and conjunctivitis [46]. Another phenomena that have bedevilled the continent are malnutrition and under nutrition, and the presence of changing climate would worsen the situation. Whereas the levels of under nutrition and malnutrition are already high across the length and the breadth of sub-Saharan Africa, projections show that with warming of 1.2 – 1.7°C by 2050, the proportion of the population that is malnourished will rise by 25-90% compared to the current [47]. According to WHO [42], under nutrition places individuals at risk of secondary or indirect health implications by amplifying vulnerability to other ailment. It is worthy to note that the repercussions of climate change on agriculture are projected to exacerbate human health conditions by affecting the affordability and accessibility of nutritious food. Outbreak of communicable diseases are likely to happen following extremities of weather events such as floods. The spread of some vector-borne diseases is anticipated to shift. For instance, it seems that malaria incidence has been disseminating into the places of high elevation in Ethiopia, Kenya, Rwanda and Burundi, where formerly it was not known IPCC [5].

Caminade *et al.* [48] argue that with regards to Sahel region, the northern periphery of the malaria prevalent strip is anticipated to swing southward by 1°C-2°C with a warming of 1.7°C by 2031-2050 as a result of an estimated fall in the duration of precipitation days in the summer. It is estimated that there is an overall rise in the incidence of malaria projection for eastern, central and southern Africa; for eastern Africa, estimations of extra population at risk under 2°C warming range from approximately 40 – 80 million and 70 – 170 million under 4°C [49]. Nevertheless, there is considerable doubt according to Chaves and Koenraadt [50] in forestalling changes in the spread of malaria due to the complexity of climate and non-climatic factors involved, with regards to air temperatures and malaria transmission fluctuating from one geographical area to another.

9. Forced Migration on the Continent of Africa

Changing climate worsens levels of poverty and unemployment as the livelihood of most people on the African continent revolve around agriculture which is predominantly rain-fed. Hertel *et al.* [51] state that urban poor are among the most susceptible to the shocks of food production that leads to jumps in food prices. According to IPCC [5], there is a projection of a rise in displacement of people under continued climate change. Tacoli [52] argues that there is complexity in factors leading to migration and such drivers comprises cultural, economic and political dynamics as well as non-climatic environmental stressors such as desertification.

The region of SSA is anticipated to be mainly impacted by movement associated with climate change-related drivers such as rise in sea-level and diminishing availability of resources as a result of shifts in climatic conditions or extremities of weather events [53]. Whereas mass population movement particularly cannot be assumed, as a matter of fact, as an adaptive response to local environmental pressures [52], it can lead to a whole set of other hazards; not only for the migrants in question but also for the populace already at the receiving region. Repercussion at the receiving site can emerge from pressures between ethnic groups, political and legal restrictions and competition for limited resources such as land [52]. Condition of livelihood in the new area of residence can place citizens at risk of different environmental hazards to those being left at home, particularly when migrants arrive to live in perilous circumstances. In a situation where sufficient sanitation and water drainage infrastructure are deficient, people might turn to rely on water supplies that can easily become contaminated and this can endanger the lives of the citizens [54].

10. Water Quality and Quantity amidst Climate Change in Africa

Majority of African citizens (290 million) are living without access to potable water as a result of inadequate physical water infrastructure, due to bad governance [7] and greedy. This implies that approximately half of world population who depend on unhygienic water for drinking are on African continent. With regards to the present trajectory, the number to persons without access to potable water is estimated to increase for the next 5 to 10 years in Africa with the exception of Northern Africa, even though the region would face rising water scarcity and likely worsening water quality too [53].

According to Welborn [7] water quality in Africa is expected to improve in some years to come, but not fast enough. The present path has it that majority of people (270 million) will lack access to quality water by 2030 and about 80 million by mid-century. Eastern part of Africa for instance is critically worrying with respects to inadequate water infrastructure. Even though climate change is anticipated to deteriorate water scarcity in the semi-arid regions of Northern and Southern Africa, Eastern Africa harbours about 112 million people (30%) of the continent's populace without access to potable water. People in Eastern Africa who lack access to drinkable water is estimated to rise to about half of population in Africa without

access to hygienic water by 2060. It is worth noting that Africa's insufficient resources invested to improved water supply also constrains development and renders adjusting to changing climate more difficult than in states with sufficient capacity [56].

11. Cost of Adaptation

Africa is at a dilemma and only crucial and speedy pragmatic actions would make it possible to effect the future repercussions of climate change and global warming. A report from World Bank suggests that it would cause third world countries a huge sum of money between US$ 75.00 and US$ 100 billion per year before such countries can adapt well to temperature change on about 2ºC by 2050 [57]. The study further stated that it would cost sub-Saharan Africa about US$ 14-17 billion, equivalent to roughly half the amount of Official Development Assistance provided for all of Africa in 2010. A report from Organisation for Economic Cooperation and Development (OECD) opines that in 2010, about US$29.3 billion was given to Africa. Some economist envisaged that in order to realise 'climate resilient' Millennium Development Goals in the sub-region, Africa will need about US$ 100 billion annually in the 2010-2020 period with about US$ 82 billion needed for standard development assistance, and an extra US$ 11-21 billion for climate change adaptation.

12. Conclusions and Recommendation

All hope is not lost for Africa. For Africa to adapt well to repercussions of climate change mishap, leaders on the continent need to improve the capacity of their citizens and put a stop to taking loans to buy expensive mansions and cars. The region is at the mercy of climate change and no one can rescue the sinking vessel of Africans as it is one of the regions which is hard hit by the impacts of climate change and variability. It is sad that the majority of the populace rely on rain-fed agriculture, and this is characterised by 'no rain no farming'. There should be diversification with regards to citizens' livelihood. Governments should subsidise agricultural inputs, irrigate arable lands, offer 'soft' loans to businessmen and women in informal sector, protect infant industries and make corruption expensive to practise. Also, there is the need for African leaders to strongly protect and, at best, expand the green vegetation on the continent. Water bodies too are to be preserved and utilised wisely as they are an endangered resource.

It is worthy to note that even if the globe decides to cut emission of greenhouse gases to zero percent (no emission), it is expected that the current concentration in the atmosphere would take not less than 100 years before it would dissipate from the atmosphere hence capacity building (adaptation) is the best option for now.

Author's Contribution

Victor Adjei contributes to conception, design, acquisition of data, analysis and interpretation of data.

Elijah F. Amaning contributes in drafting the article and reviewing it critically for significant intellectual content and gives final approval of the version to be submitted.

References

[1] Müller-Kuckelberg. Climate Change and Its Impact on the Livelihood of Farmers And Agricultural Workers In Ghana. 2012.

[2] United Nations Secretary-General, Secretary-General's press encounter on climate change, 29 March 2018, https:// www.un.org/sg/en/content/sg/press-encounter/2018-03-29/ secretary-generals-press-encounter-climate-change-qa.

[3] Romm, J. Climate change: what everyone needs to know, New York: Oxford University Press, 2018, 7.

[4] IPCC. Stabilisation of atmospheric greenhouse gases: physical, biological and socioeconomic implications, IPCC Technical paper 3,WMO, UNEP 1997b

[5] IPCC Summary for policymakers. In: Climate change 2014: Impacts, adaptation, and vulnerability. Part A: Global and sectoral aspects. Contribution of Working Group II to the Fifth Assessment Report of the Intergovermental Panel on Climate Change [Field CB, Barros VR, Dokken DJ, Mach KJ, Mastrandrea MD, Bilir TE, Chatterjee M, Ebi YL, Estrada YO, Genova RC, Girma B, Kissel ES, Levy AN, MacCracken S, Mastrandrea PR, White LL (eds)]. Cambridge University Press, Cambridge, UK and New York, USA. 2014. pp 1–32

[6] Krause, F., Bach, W. and Koomey, J. Energy Policy in the Greenhouse, Volume 1: From Warming Fate to Warming Limit. Benchmarks for a Global Climate Convention. International Project for Sustainable Energy Paths. El Cerrito, California. 1989

[7] Welborn, J. Africa and climate change Projecting vulnerability and adaptive capacity. Institute for Security Studies, 2018

[8] Warren, R. Role of interactions in a world implementing adaptation and mitigation solutions to climate change, The Royal Society, 234, https://doi.org/10. 2010

[9] National Oceanic Atmospheric Administration (NOAA). Climate at a glance: global time series.

NOAA National Centres for Environmental information. (Retired on June, 2021). 2018.

[10] Seneviratne S.I., Nicholls, N., Easterling, D. et al. Changes in climate extremes and their impacts on the natural physical environment. In: Field CB, Barros V, Stocker TF et al (eds) Managing the risks of extreme events and disasters to advance climate change adaptation. A special report of working groups I and II of the Intergovernmental Panel on Climate Change. 2012. pp 109–230.

[11] Kirtman B, Power SB, Adedoyin JA et al. Near-term climate change: projections and predictability. In: Stocker TF, Qin D, Plattner G-K et al (eds) Climate change 2013: the physical science basis, Contribution of Working Group I to the Fifth Assessment Report of the Intergovernmental Panel on Climate Change. Cambridge University Press, Cambridge, UK. 2013

[12] Hartmann, D. L., Klein Tank, A. M. G., Rusticucci, M., Alexander, L. V., Brönnimann, S., Charabi, Y., Dentener, F. J., Dlugokencky, E. J., Easterling, D. R., Kaplan, A., Soden, B. J., Thorne, P.W., Wild, M. & Zhai, P. M. (2013). Observations: Atmosphere and surface. In: T. F. Stocker, D. Qin, G.-K. Plattner, M. Tignor, S. K. Allen, J. Boschung, A. Nauels, Y. Xia, V. Bex & P. M. Midgley (Eds.), Climate Change (2013). The Physical Science Basis. Contribution of Working Group I to the Fifth Assessment Report of the Intergovernmental Panel on Climate Change. Cambridge, United Kingdom and New York, NY, USA: Cambridge University Press.

[13] Adjei, V. & Kyerematen, R. Impacts of Changing Climate on Maize Production in the Transitional Zone of Ghana. *American Journal of Climate Change,* 2018.7, 463-476. https://doi.org/10.4236/ajcc.2018.73028

[14] Adjei, V., Anlimachie, M.A & Ativi, E.E. (2020). Understanding the Nexus between Climate Change, the Shift in Land Use toward Cashew Production and Rural Food Security in Ghana; the Experiences of Farmers in the Transition Zone of Ghana. *Journal of Atmospheric Science Research.*

[15] Girvetz E. H., Zganjar C. Dissecting Indices of Aridity for Assessing the Impacts of Global Climate Change. 2014. 126:469–483

[16] New M, Porter J.R., Xie L. et al. Evidence of trends in daily climate extremes over southern and West Africa. J Geophys Res 111:D14102.https://doi.org/10.1029/ 2006 JD006289

[17] IPCC. Summary for policymakers. In: Field CB, Barros V, Stocker TF et al (eds) Managing the risks of extreme events and disasters to advance climate change adaptation, A Special Report of Working Groups I and II of the Intergovernmental Panel on Climate Change. Cambridge University Press, Cambridge, UK. 2012

[18] Girvetz E. H, Zganjar C, Shafer S. et als. Applied climate-change analysis: the Climate Wizard tool. 2009 PLoS One 4(12):e8320

[19] Sillmann, J., Kharin, V.V., Zhang X. et al. Climate extremes indices in the CMIP5 multimodel ensemble: part 1. Model evaluation in the present climate. J Geophys Res Atmos, 2012, 118:1716– 1733. https://doi.org/10.1002/jgrd.50203

[20] Ramirez-Villegas J., Challinor, A.J., Thornton P.K. et al. Implications of regional improvement in global climate models for agricultural impact research. Environ Res Lett, 2013. 8:24018

[21] Niang, I., Ruppel O.C., Abdrabo M.A., Essel, A., Lennard C., Padgham J., Urquhart, P. Africa. In: Climate change 2014: impacts, adaptation and vulnerability. Contribution of Working Group II to the Fifth Assessment Report of the Intergovernmental Panel on Climate Change. Cambridge University Press, Cambridge.UK, 2014.

[22] Vizy, E. K., & Cook, K. H. Mid-twenty-first-century changes in extreme events over northern and tropical Africa. Journal of Climate, 2012, 25(17), 5748–5767. doi:10.1175/JCLI-D-1100693.1.

[23] Patricola, C.M. & Cook, K.H. Northern African climate at the end of the twenty-first century: an integrated application of regional and global climate models. Climate Dynamics, 2010, 35(1), 193-212.

[24] Sylla, M. B., Gaye, A. T., & Jenkins, G. S. On the fine-scale topography regulating changes in atmospheric hydrological cycle and extreme rainfall over West Africa in a regional climate model projections. *International Journal of Geophysics,* 2012*, 981649. doi:10.1155/2012/ 981649.*

[25] Haensler, A., Saeed, F., & Jacob, D. Assessing the robustness of projected precipitation changes over central Africa on the basis of a multitude of global and regional climate projections. Climatic Change, 2013, 121(2), 349–363. doi:10.1007/10584-013-0863-8.

[26] Sylla, M. B., Elguindi, N., Giorgi, F., & Wisser, D. Projected robust shift of climate zones over West Africa in response to anthropogenic climate change for the late 21st century. Climatic Change, 12016, 34(1), 241–253. doi:10.1007/s10584-015-1522-z.

[27] Po¨rtner H-O, Karl, D.M., Boyd P.W., Cheung, W.W.L., Lluch-Cota, S.E., Nojiri Y., Schmidt D.N., Zavialov, P.O. Ocean systems. In: Climate change 2014: Impacts, adaptation, and vulnerability. Part A:

global and sectoral impacts. Contribution of Working Group II to the Fifth Assessment Report of the Intergovernmental Panel on Climate Change. Cambridge University Press, Cambridge, U.K., and New York, U.S, 2041.

[28] Müller C, Cramer W., Hare W.L. et al. Climate change risks for African agriculture. Proc Natl Acad Sci., 2011, https://doi.org/10.1073/pnas.1015078108

[29] Rippke, U., Ramirez-Villegas J., Jarvis, A. et al. Timescales of transformational climate change adaptation in sub-Saharan African agriculture. Nat Climte Change, 2016 6(6):605–609

[30] Ramirez-Villegas, J., Thornton P.K. Climate change impacts on African crop production, CCAFS Working Paper no. 119. CGIAR Research Program on Climate Change, Agriculture and Food Security (CCAFS), 2015, Copenhagen (retrieved on May, 2021)

[31] Myers, S.S., Zanobetti, A., Kloog, I., Huybers, P., Leakey, A.D.B., Bloom, A.J., Carlisle, E., Dietterich, L.H., Fitzgerald, G., Hasegawa, T., Holbrook, N.M., Nelson, R.L., Ottman, M.J., Raboy, V., Sakai, H., Sartor, K.A., Schwartz, J., Seneweera, S., Tausz, M. & Usui, Y. Increasing CO_2 threatens human nutrition. *Nature*, 2014, 510(7503): 139–142.

[32] Medek D.E., Schwartz J., & Myers S.S. Estimated effects of future atmospheric CO_2 concentrations on protein intake and the risk of protein deficiency by country and region. Environ Health Perspect, 2017, 125(8):087002

[33] Centre for International Governance Innovation (2009). Climate Change in Africa: Adaptation, Mitigation and Governance Challenges.

[34] Smit B. et al., Climate change: impacts, adaptation, and vulnerability, IPCC, 2001, 894, www.ipcc.ch/ipccreports/ tar/wg2/pdf/wg2TARchap18

[35] World Bank. Turn down the heat: climate extremes, regional impacts, and the case for resilience. Extremes_Regional_Impacts_Case_for_Resilience_Print%20 version_FINAL.pdf, 2013.

[36] Adjei V. & Kwantwi Boafo L. Maize and Cashew Farming in the Face of Climate Change Variability in the Transitional Zone of Ghana: A Case Study of Nkoranza South Municipality. *American Journal of Environmental Sciences, USA* 2019, DOI: 10.3844/ajessp.

[37] Food and Agriculture Organisation. An Introduction to the Basic Concepts of Food Security. Food Security Information for Action Practical Guides. Rome, FAO. 2008

[38] Adjei & Alorm. Cashew Production as a Climate Change Adaptation and Mitigation Tool for Agriculture. Advances in Earth and Environmental Science (2020). www.unisciencepub.com

[39] United Nations. Food security in Africa: learning lessons from the food crisis. United Nations Conference on Trade and Development, 2009.

[40] McMichael AJ, Lindgren E. Climate change: present and future risks to health, and necessary responses. J Intern Med, 2011, 270(5):401–413. doi:10.1111/j.1365-2796.2011.02415.x Midgley GF

[41] WHO. Protecting health from climate change: connecting science, policy and people. World Health Organization, Geneva, 2009, pp 1–36

[42] Smith, K.R., Woodward, A., Campbell-Lendrum, D., Chadee, D.D., Honda, Y., Liu, Q., Olwoch, J.M., Revich, B., Sauerborn, R. Human health: impacts, adaptation and co-benefits. In: Climate change 2014: Impacts, adaptation and vulnerability. Contribution of Working Group II to the Fifth Assessment Report of the Intergovernmental Panel on Climate Change. Cambridge University Press, Cambridge, U.K., and New York, US. 2014

[43] Azongo D.K., Awine T., Wak G., Binka F.N., Oduro A.R. (2012). A timeseries analysis of weather variability and all-cause mortality in the Kasena-Nankana Districts of Northern Ghana, 2012, 1995–2010. Glob Health Action. doi:10.3402/gha.v5i0.19073

[44] Codjoe S.N.A., & Nabie V.A. Climate Change and Cerebrospinal Meningitis in the Ghana Belt. *International Journal of Environmental Research and Public Health,* 2014. *(*6923-6939)

[45] Patz, J.A., Olson S.H., Uejo C.K., Gibbs, H.K. Disease emergence from global climate and land use change. Med Clin North Am, 2008. 92:1473–1491. doi:10.1016/j.mcna.2008.07.007

[46] Lobell D.B., Schlenker W., Costa-Roberts J. Climate trends and global crop production since 1980. Science, 2011. 333(6042):616–620. doi:10.1126/science.1204531

[47] Caminade C., Ndione, J.A., Kebe .CM.F., Jones, A.E., Danuor, S., Tay, S., Tourre, Y.M., Lacaux J.P., Vignolles C., Duchemin J.B., Jeanne I, Morse A.P. Mapping Rift Valley fever and malaria risk over West Africa using climatic indicators. Atmos Sci Lett, 2011, 12:96–103. doi:10.1002/asl.296

[48] Caminade C, Kovats S, Rocklov J, Tompkins AM, Morse AP, Colo ´nGonza ´lez FJ, Stenlund H, Martens P, Lloyd SJ (2014). Impact of climate change on global malaria distribution. Proc Natl Acad Sci USA 111(9):3286–3291. doi:10.1073/pnas. 1302089111

[49] Chaves LF, Koenraadt CJM (2010) Climate change

and highland malaria: fresh air for a hot debate. Q Rev Biol 85(1):27–55. doi:10.1086/650284

[50] Hertel, T.W., Burke, M. B., & Lobell, D.B. (2010) The poverty implications of climateinduced crop yield changes by 2030. Global Environmental Change,20(4), 577585.

[51] Tacoli, C. (2009). Crisis or adaptation? Migration and climate change in a context of high mobility. Environ Urban 21:513–525. doi:10.1177/0956247809342182

[52] Gemenne F (2011.) Why the numbers don't add up: a review of estimates and predictions of people displaced by environmental changes. Glob Environ Change 21(S1):S41–S49. doi:10.1016/j. gloenvcha.2011.09.005

[53] Douglas I, Alam K, Maghenda M, Mcdonnell Y, Mclean L., Campbell J (2008). Unjust waters: climate change, flooding and the urban poor in Africa. Environ Urban 20(1):187–205. doi:10.1177/0956247808089156

[54] WHO/UNICEF (2017). Progress on drinking water, sanitation and hygiene, Joint Monitoring Programme on Water and Sanitation, http://www.who.int/mediacentre/ news

[55] O'Neill B. C et al., (2017). The roads ahead: narratives for shared socioeconomic pathways describing world futures in the 21st century, *Global Environmental Change*, 42, https://doi. org/10.1016/j.gloenvcha.2015.01.004.

[56] UNEP (2012). Climate Change Challenges for Africa: Evidence from selected Eu-Funded Research Projects: www.unep. org/research4policy.

BILINGUAL PUBLISHING CO.
Pioneer of Global Academics Since 1984

Journal of Atmospheric Science Research
https://ojs.bilpublishing.com/index.php/jasr

ARTICLE

Simplified Equation Models for Greenhouses Gases Assessment in Road Transport Sector in Burkina Faso

Tiga NEYA[1,2,3*] Galine YANON[3] Mouhamadou Bamba SYLLA[4] Oble NEYA[5] Julien W. SAWADOGO[6]

1. University of Joseph Ki-Zerbo Ouagadougou, Burkina Faso
2. Ministry of Environment Green Economy and Climate Change Ouagadougou, Burkina Faso
3. Global Green Growth Institute, Ouagadougou, Burkina Faso
4. African Institute for Mathematical Sciences, Kigali, Rwanda
5. West African Climate Change and Land Use, Ouagadougou, Burkina Faso
6. University of Augsburg, Germany

ARTICLE INFO

Article history
Received: 24 September 2021
Accepted: 12 October 2021
Published: 20 October 2021

Keywords:
GHG emission
Transport sector
Modelling

ABSTRACT

Transport sector is cited among the key emitted sector. In Burkina Faso, road transport occupies more than 60% of the emissions of the entire transport sector. However, there is no model equation for greenhouse gases modelling in transport sector. A methodology combining literature review and survey has been adopted to develop the simplified model equation in transport sector. The vehicle type survey allowed the identification of the type of vehicle and the literature review allowed the identification of the key parameters used for greenhouses gases modelling. The results revealed 10 vehicle types for road transport in Burkina Faso such as: Private cars, Public Transport/Buses, Special Vehicle (Ambulances, Fire bus, Funeral vehicles), other vehicle, Motorcycles, Wheeler, Rail, Van, Lorries and Truck Tractor. The keys parameters for greenhouse gases modelling are Fleet availability, Average annual distance travelled, Fuel Economy and Fuel emission factor. For all vehicle type identified simplified model equation was developed to support Burkina Faso, assessing greenhouse gases emission in the sector of transport. This approach could be replicated in other countries in the sub-Saharan Region.

1. Introduction

Burkina Faso's geographic position, at the center of Sudano-Sahelian zone in West Africa, makes it particularly vulnerable to the adverse effects of climate variability and change. Burkina Faso's economy is essentially based on a rainfed agriculture (plant and animal production) which contribute mostly to the country Gross Domestic Product (GDP). According to the national statistic and demography agency data, the population is growing at the rate of about 2.4 % per year; and 46,4% of the populations (11,849,520 habitants among which 51,1% are women)

*Corresponding Author:
Tiga NEYA,
University of Joseph Ki-Zerbo Ouagadougou, Burkina Faso; Ministry of Environment Green Economy and Climate Change Ouagadougou, Burkina Faso; Global Green Growth Institute, Ouagadougou, Burkina Faso;
Email: neyatiga@gmail.com

DOI: https://doi.org/10.30564/jasr.v4i4.3758

lives below the poverty line, estimated at 82,672 FCFA in 2004 (US $ 165).

Over the past two decades, Burkina Faso has suffered from the adverse effects of the climate. The most important among these climatic shocks are droughts due to insufficient rainfall and its uneven distribution, floods from exceptional heavy rains, heat waves and intense dust layers. The persistence of climate change will inevitably lead to an increase in the frequency and magnitude of extreme weather events; their repercussion in terms of impacts will be detrimental to certain sectors and to socio-professional strata with limited means. As the country is potentially vulnerable to projected climatic shocks, it urges to develop adaptation and mitigation measures.

Reducing greenhouse gases to fight against the adverse effects of climate change is one of the world's major development challenges [1-3]. The increase in atmospheric carbon dioxide (CO_2) is cited as the main factor and cause of global warming and is attributed, in large part, to human activities [4]. To address these observed global challenges, all 195 members' countries of the United Nations Framework Convention on Climate Change (UNFCCC) have committed to reduce their greenhouse gas emissions to stabilize the increase in global terrestrial temperature to 2°C through their commitment materialized in a Nationally Determined Contribution (NDC) in Paris in 2015. Since then, the Paris Accord reiterated the wish that every member country of the UNFCCC should submit a revised Determined Contribution at the national level every five years, and more ambitious than the previous NDCs; to effectively contribute to this global effort of fighting against the negatives effects of climate change, through a significant reduction of greenhouse gas emissions into the atmosphere.

Burkina Faso's contribution to the fight against the effects of climate change on natural, economic, and human systems has been materialized by the ratification of the United Nations Framework Convention on Climate Change (UNFCCC) in 1993 as well as its implementing texts; the signing of the Paris Agreement on Adaptation to Climate Change in 2015. Thus, to better contribute to the global effort of greenhouse gas reduction, Burkina Faso as UNFCCC member country, and signatory to the Paris Agreement in 2015, has submitted its nationally determined contribution (NDC) in 2015. Burkina Faso has committed to reduce his greenhouse gas emissions by about 6% through its unconditional scenario and about 11.6% through its conditional scenario. After five years of implementation of the first generation of Burkina Faso's NDC, the year 2020 marks the deadline for revising the reviewed NDCs in accordance with the provisions of the Paris Agreement adopted in 2015. It is in this global context of NDC revision that Burkina Faso is resolutely committed to reviewing its Nationally Determined Contribution, to comply with the requirements and recommendations of the Paris Agreement. As the principle and objective of revising the NDCs is to revise the greenhouse gas emission reduction targets upwards, it was necessary that the GHG reduction potential of the actions to be included in Burkina Faso's new NDC be assessed to enable Burkina Faso to set new ambitious, realistic, and achievable targets.

However, it is important at mention that at this moment, there is no greenhouses gas model to enable technician/ practitioners to easily assess capacities in term of GHG reduction. The present paper will provide interesting elements to support the prioritization of actions with high GHG reduction potential to be included in the NDC and to help decision-makers to make strategic choices, improving their contribution to the international effort of stabilizing the earth's temperature in the range of 1.5 to 20 C. Therefore, to better support this objective, it become urgent, the establishment of a greenhouse gas modelling for the sector of Transport. The model will support and help practitioners in their everyday work.

2. Materials and Method

2.1 Vehicle Type Identification

To identify the type of vehicle 10 years' time series data of vehicle from 2010 to 2020 were collected through the statistical office of the Ministry of Transport urban mobility and Road Secure of Burkina Faso. For each time series the type of the vehicle was recorded in order to establish a complete list of vehicles imported in Burkina Faso. To get a broad idea on vehicle number increasing, Gross Domestic Product (GDP) elasticity (0.8) and average (3.47%) from historical data have been used. For that 2017 was used as baseline year given the availability of data to cover the analysis.

2.2 Greenhouses Gas Model Development

For each type of vehicle identified, a specific model was developed using the general Equation (1)

$$E = N \times D \times F \times E_f \times \frac{A}{100} \quad (1)$$

Where :

-N: Number of vehicle in given type of vehicle

-D: Annual average travelled distance in (Km)

-F: Fuel economy per type of vehicle (Liter/100 Km)

-Ef: Emission factor of fuel type.

-A: Fleet availability /Availability of the vehicle or percentage of vehicle use (%)

For all parameters in greenhouses gases modelling, Fuel economy, Emission factor of fuel type and vehicle availability were considered as constant parameters while only Number of vehicle and Annual average travelled distance were variable parameters. All the constants parameters were obtained through literatures reviews and previous published works within the country, in West Africa and over the world [5,6].

2.3 Greenhouses Gas Vehicle Model Calibration and Validation

For model's calibration and validation, data from 2017 were used as baseline year according to the availability of data. Moreover, fuel consumption data used for 2018 National greenhouse gases inventory in transport sector were used to calibrate and validate the model. The testing and calibration allowed performing each model per type of vehicle.

3. Results and Discussions

3.1 Vehicle Type in Burkina Faso

In Burkina Faso 10 vehicles types were identified in road transport sector (Table 1).

Table 1. type of vehicle identified following the Ministry of Transport classification in Burkina Faso

N0	Type of vehicle	Observation
01	Private cars	Widely uses
02	Public Transport - Buses	Minority uses
03	Special Vehicle	Minority uses
04	Other vehicle	Minority uses
05	Motor Cycles	Minority uses
06	Wheeler	Minority uses
07	Rail	Minority uses
08	Van	Average uses
09	Lorries	Average uses
10	Truck Tractor	Minority uses

3.2 Projection in the Number of Vehicles, Per Type, from 2017 to 2040

Vehicles trend analysis shown a huge increase in motorbikes from 2.3 million in 2017 to 7.7 million in 2040 (Figure 1).

The exponential increasing of motorbike could contribute to the worsening of air pollution in the country and lead to some disease development and climate change. The World Health Organization (WHO) estimates that urban air pollution contributes to approximately 800,000 deaths per year in the world [7] and the principal gases affecting human health are among other PM10; Nitrogen Dioxide (NO_2); Sulphur Dioxide (SO_2) and O_3 and are more generated by transport sector. However In Burkina Faso the average NO_2 concentration increased from 24.9 µg/m^3 in 2007 to 94.7 µg/m^3 in 2012 [8-10]. The PM10 concentration has also increased from 1800 µg /m^3 in 2007 to about 2800 µg /m^3 in 2019 [11] and will become worse in the future given the vehicle and motorbike park increasing rate.

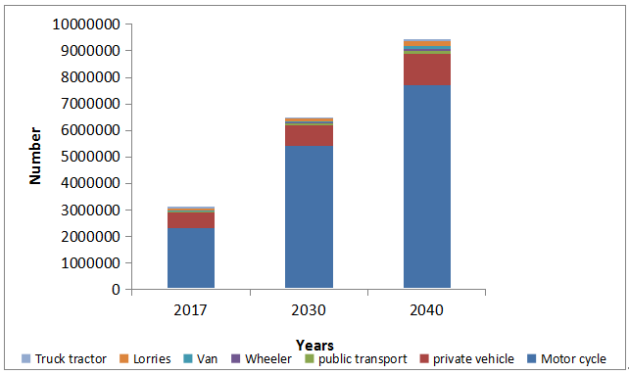

Figure 1. Vehicle number.

Source: data source from the survey

3.3 Values of Constant Parameters Used

For each vehicle type five parameters were used to calibrate the model using the baseline year data of 2017 (Table 2).

Table 2. type of vehicle and constant parameters used for Greenhouses gases modelling calibration and Validation.

Type of vehicle	Type of fuel	Fleet availability (%)	km/vehicle/ year	Fuel Economy - L/100km	Emission F - kgCO2e/ L
Private cars	gasoline	0.75	15 000	9	2.62
Public Transport - Buses	Diesel	0.66	20000	40	2.77
Special Vehicle	Diesel	0.75	10000	15	2.77
Other vehicle	Diesel	0.75	10000	15	2.77
Motor Cycles	Gasoline	0.75	7000	2	2.62
Wheeler	Gasoline	0.75	7000	5	2.62
Rail	Diesel	-	-	11.6	2.77
Van	Diesel	0.66	30000	15	2.77
Lorries	Diesel	0.66	30000	25	2.77
Truck tractor	Diesel	0.66	40000	30	2.77

Among the recorded parameters only gasoline emission

factor has been developed in Burkina Faso [12] the other parameters are default value developed by previous work outside the country [4,13].

3.4 Vehicle Type Model for Greenhouses Gases Assessment in Road Transport Sector

3.4.1 Private Vehicle Model Equation

The model for private vehicle CO2 equivalent assessment is given by Equation (2).

$$E_{pc}(Teqco_2) = (1.7685 D_{PC} \sum N_{Pc}) 10^{-10} \quad (2)$$

Where $E_{Pc:}$ CO_2 equivalent emitted by private vehicle
N_{pc}: Number of private vehicle
D_{Pc}: Average annual distance travelled

3.4.2 Special Vehicle Model Equation

The model for Special vehicle CO_2 equivalent assessment is given by Equation (3).

$$E_{Sv}(Teqco_2) = (3.11625 D_{Sv} \sum Nv) 10^{-10} \quad (3)$$

where E_{Sv}: CO_2 equivalent emitted by Special vehicle
N_{Sv}: Number of Special vehicle
D_{Sv}: Average annual distance travelled

3.4.3 Public Transport - Buses Model Equation

The model for Public Transport/Buses CO_2 equivalent assessment is given by Equation (4).

$$E_{Pt}(Teqco_2) = (7.3128 D_{Pt} \sum Nt) 10^{-10} \quad (4)$$

where $E_{Pt:}$ CO_2 equivalent emitted public transport / buses
$N_{Pt:}$ Number of public transport/buses
$D_{Pt:}$ Average annual distance travelled

3.4.4 Van Model Equation

The model for Van CO_2 equivalent assessment is given by Equation (5).

$$E_v(Teqco_2) = (2.7423 D_v \sum Nv) 10^{-10} \quad (5)$$

E_V: CO_2 equivalent emitted Van
N_V: Number of Van
D_V: Average annual distance travelled

3.4.5 Lorries Model Equation

The model for Lorries CO_2 equivalent assessment is given by Equation (6).

$$E_L(Teqco_2) = (4.5705 D_L \sum N_L) 10^{-10} \quad (6)$$

where E_L; CO_2 equivalent emitted Lorries
N_L: number of Lorries
D_L: Average annual distance travelled

3.4.6 Motor Cycles Model Equation

The model for Motor Cycles CO_2 equivalent assessment is given by Equation (7).

$$E_{Mc}(Teqco_2) = (3.93 D_{Mc} \sum N_{Mc}) 10^{-11} \quad (7)$$

Where E_{Mc}: CO_2 equivalent emitted Motor Cycles
N_{Mc} number of motor-cycle
D_{Mc}: Average annual distance travelled

3.4.7 Wheeler Model Equation

The model for Wheeler CO_2 equivalent assessment is given by Equation (8).

$$E_w(Teqco_2) = (9.825 D_w \sum N_w) 10^{-11} \quad (8)$$

Where : E_W: CO_2 equivalent emitted wheeler
N_W Number of wheeler
D_W: Average annual distance travelled (Km)

3.4.8 Truck Tractors Model Equation

The model for Truck Tractors CO_2 equivalent assessment is given by Equation (9).

$$E_{Tr}(Teqco_2) = (5.4846 D_{Tr} \sum N_{Tr}) 10^{-10} \quad (9)$$

Where E_{Tr}: CO_2 equivalent emitted from truck tractor
N_{Tr}: Number of Truck Tractor
D_T: Average annual distance travelled (Km)

3.4.9 Other Vehicle Model Equation

The model for Truck Tractors CO_2 equivalent assessment is given by Equation (10).

$$E_{Ov}(Teqco_2) = (3.11625 D_{Ov} \sum N_{Ov}) 10^{-10} \quad (10)$$

Where E_{Ov}: CO_2 equivalent emitted from other vehicle
N_{Ov}: Number of other vehicle
D_{Ov}: Average annual distance travelled (Km)

3.5 Potential of Greenhouses Gases Emission

3.5.1 Greenhouse Gases Emission Per Type of Vehicle

The application of the formulas above leads to the fol-

lowing values of GHG emissions for the transportation sector for the reference year 2017:

Table 3. Amount of CO_2 emitted for the base year 2017 (in $MtCO_2eq$)

Vehicle type	Amount of GHG emitted ($MtCO_2eq$)
Motorbike	0.64
Private cars	0.63
Public Transport /Buses	0.18
Three-wheeler	0.01
Pickup/Van	0.36
Truck/Lorries	0.44
Trucks (cabs)	0.52
Road Passenger	1.47
Road Freight	1.32
Rail	0.03
Total	2.82

3.5.2 BAU Greenhouses Gases Emission Scenario Projections

With the various elements of emissions projections prepared for the BAU scenario, results can be simulated, starting with the baseline year 2017 and historical trends (growth rates). The results of the projections are presented up to 2040, which is the target year used in this study (Figure 2).

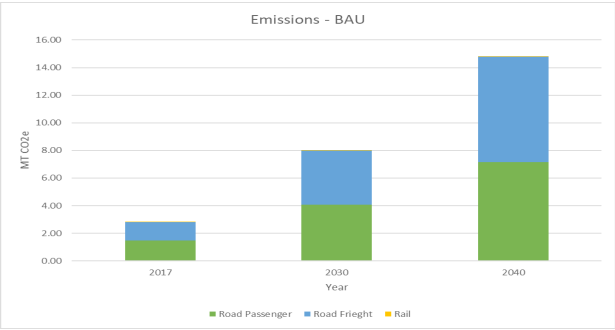

Figure 2. Evolution of GHGs emissions in transport sector from 2017 to 2040

The model shows that BAU emissions will increase from 2.82 MT in 2017 to 8.04 MT in 2030 and to 14.84 MT in 2040 (Figure 3). It should be noted that this figure is higher than the current CDN forecast (6.9 MT in 2030). However, the current NDC is solely based on fuel data and an assumption of 8% annual emissions growth. In addition, the current NDC includes aviation emissions with the assumption of increasing emissions from rail transport, unlike the present analysis which excludes aviation and assumes a constant evolution of rail emissions, due to the difficulties in deriving a future trend in rail fuel consumption from the available data.

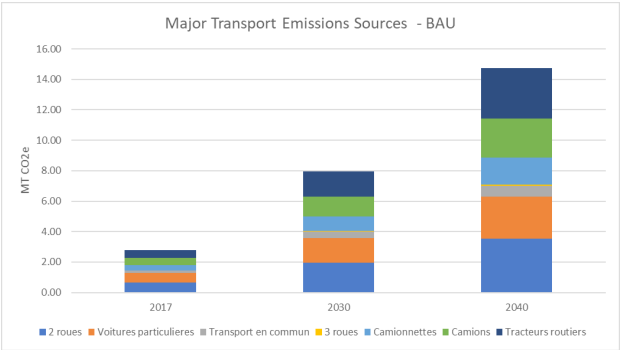

Figure 3. Contribution to Transport GHG Emissions by Vehicle Type from 2017 to 2040

Most of the sector's emissions come from freight transport vehicles (trucks and road tractors) with about 40% of total emissions. This mode is followed by 2-wheelers, which account for 25% of emissions, then by passenger cars (18%). 1These contributions show the need for an approach that addresses both passenger and freight vehicle emissions through the implementation of options that would absorb and reduce the growing volumes of the concerned vehicle types traffic, as shown in Figure 4 and Figure 5, where we see a considerable increase in the number of motorbike from 2.3 million in 2017 to 7.7 million in 2040 and passenger vehicles from 238,551 in 2027 to 626,042 in 2040.

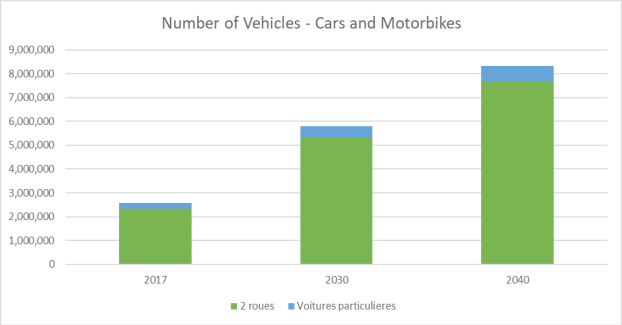

Figure 4. Evolution of vehicles number from 2017 to 2040

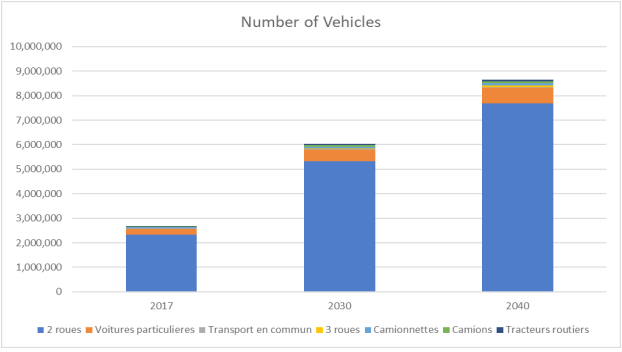

Figure 5. Evolution of vehicle fleet by type from 2017 to 2040

As shown in Figure 5, the volume of motorbikes dwarfs other modes of transport. But it is important to remember that in terms of relative contribution to total emissions - as mentioned previously - an approach from government to tackle all forms of emissions (from passengers and freight) will be needed.

It is also important to note that the problem of air quality arises in Ouagadougou. This situation will worsen in the future and requires further analysis on the issue. Air pollution has become a major concern because of its adverse effects on the environment (climate change) and human beings (health problems). According to the World Health Organization, urban air pollution contributes to about 800,000 deaths per year worldwide [7], and the main gases affecting human health include PM_{10}, NO_2, SO_2, and O_3, which are generated more by the transport sector. For Burkina Faso, the average NO_2 concentration has increased from 24.9 µg/m^3 in 2007 to 94.7 µg/m^3 in 2012. PM_{10} concentration also increased from 1,800 µg /m^3 in 2007 to about 2,800 µg /m^3 in 2019 [12]. The results of projections of future changes in vehicle ownership show that this problem will worsen in the future, if public transport policies or cleaner forms of transport are not introduced.

The results are consistent with those observed in other Asian cities and lead to major challenges in terms of air quality and road congestion, on the assumption that trends in GNI and hence in vehicle ownership would increase at historical rates. If GNI per capita were to increase (even at an average of 7 percent per year), traffic would grow at an even faster rate (see box on Vietnam).

It was not possible to predict the evolution of rail consumption due to lack of data. The analysis of existing data has showed a decreasing trend in fuel consumption, which motivated the choice of a constant evolution assumption in rail emissions compared to the 2017 level. The change in rail transport fuel consumption over the period 2010-2017 is shown in Figure 6:

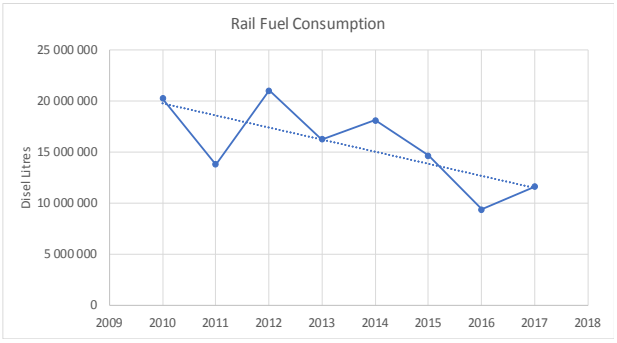

Figure 6. Change in rail transport fuel consumption from 2010 to 2017

3.6 Comparison with Viet Nam - Should GDP Increase Much Faster than 3.4%

Viet Nam is one of the world's development success stories, with rapid economic development since the 1990s, due to market reforms and the end of the US-led trade embargo. During this time GDP per capita has increased from US $96 in 1990 to US $ 2,715 in 2019, with subsequent dramatic falls in poverty, and increases in life expectancy, literacy, and numeracy. During this time, vehicle ownership has sky-rocketed, with the number of motorbikes having increased 48-fold over the last three decades, from 1.2 million in 1990 to over 58 million in 2018, according to the Department of Traffic Safety at the Ministry of Transport. The two major cities of Hanoi and Ho Chi Minh City (HCMC) have the largest number, with nearly 6 million and 8.5 million, respectively. This rise in vehicle ownership has brought about several challenges in deteriorating air quality and traffic congestion. Indeed, Hanoi has the ominous record of being the second-worst city in South East Asia for air quality and even recorded an unprecedented level of 385 on the AQI in 2019, with road traffic being one of the major causes (along with coal fired power stations, heavy industry and agricultural emissions).

The case of Viet Nam offers a warning and an opportunity for Burkina Faso, Burkina Faso is at a similar development stage to what Viet Nam was in the late 1990s, and like Viet Nam, there exists aspirational demand for vehicle ownership, in particular that of motorbikes. Though our analysis has shown that motorbike ownership will grow to from 0.11 in 2017 to around 0.25 per person in 2040 (assuming a population of 30 million in 2040), Viet Nam today has around 0.6 bikes per person (58 million bikes per 96 million people) - so even though the 7.7 million bikes predicted by our model in 2040 for Burkina Faso looks large, the stark reality is that this could be a large underestimation. Should Gross Domestic Product (GDP) growth advance at a faster rate, which would be very desirable, and the government fail to invest in public transportation, Ouagadougou, like Hanoi and HCMC today, could be beset with air quality and road traffic problems.

There exists a golden opportunity to prioritize public transportation that is fast, green, efficient and affordable that is backed up by the correct policy environment, to encourage as many Burkinabe to take public transport over their motorbike or car.

4. Conclusions

There is somewhat of a "time bomb" of emissions in the motorbikes and the preference for this as the preferred

mode of transport. Without the correct government policies, including supporting public transport, we can expect a dramatic increase in motorbike ownership from today's levels bringing with its air quality and congestion issues. And the lack of investment in rail will push more and more freight into trucks, further increasing emissions.

The results from this study help to close the existing knowledge gap with respect to Greenhouses gases estimation in road transport sector. It will help developing countries to easily assess their yearly Greenhouses gases emission in transport sector and to meet the IPCCC 2006 guidelines for tier 2. The simplified model equation will be used as decision making tool to guide decision maker in developing and implementing a low emissions action in the transport sector. Given the fact that the simplified models equation has been established using secondary and default data. We recommends that following work to come out with specific parameters to increase the accuracy on greenhouses gases estimation in the road transport sector (i) survey on KMs travelled per year and fleet availability in Burkina Faso and overs West Africa, (ii) establishment of specific emission factor of Gasoline and Diesel fuel and (iii) survey on Fuel economy information in Burkina Faso and over west Africa. Better data would strengthen the model, for example on average KMs driven and fuel economy of vehicles. These data should be collected via surveys and can be fed into the model in future.

Authors' Contributions

This work was carried out in collaboration between all authors. TN designed the study, performed the statistical analysis, and wrote the first draft of the manuscript. GY, BY, ON and SW and guided the design of the study and supervised data collection and analyses of the study.

Funding

"This research was funded by Global Green Growth Institute , through his Monitoring , Reporting and Verification National Project in order to highlight Transport sector contribution to National Greenhouses emission".

Conflict of interests

Authors have declared that no competing interests exist.

Acknowledgments

I am indebted to many individuals in assuring the completion of this study. First and foremost, my gratitude to the Ministry of Environment Green Economy and Climate Change who provided technical, logistical and additional financial support. I would like to extend my gratitude specifically to: My supervisors Dr Augustin KABORE, The Permanent Secretary of National Sustainable Development Council, whose accepted to support and facilitate the interaction with the key stakeholders and Special thanks to Capacity Building Initiative for climate Transparency for helping to organize stacjholders meeting in order to collect data.

I also thanks all my colleagues for this enthusiasm during three years that we spent together. Finally, I am also grateful to my wife Rahinatou NACRO and my children Achad NEYA and Kader NEYA, for supporting me in prayers, and by way of encouragement. Finaly, I am grateful to Hypolite TIENDREOBGO, Yacouba MOUNI both research assistants for their efforts and professionalism which were instrumental to the success of this study.

References

[1] IPCC. 2007: Climate Change: Synthesis Report. Contribution of Working Groups I, II and III to the Fourth Assessment Report of the Intergovernmental Panel on Climate Change. Geneva: Intergovernmental Panel on Climate Change, 52 p.

[2] Paris. 2015: Adoption of the Paris Agreement Proposal by the President, 21932(December), 1-32.

[3] Neya T., Neya O. Abunyewa, A.A. et al. 2020: Carbon sequestration potential and marketable carbon value of smallholder agroforestry parklands across climatic zones of Burkina Faso: current status and way forward for REDD+ implementation. Environmental Management Springer.
DOI: 10.1007/s00267-019-01248-6.

[4] Lindzen, R. 2009: On the observational determination of climate sensitivity and its implications, (August), 19-23.

[5] Mutenyo, J., Banga, M., Matovu, F., Kimera, D., Lawrence, K. (2015). Baseline survey on Uganda's national average automotive fuel economi. http://staging.unep.org/Transport/ new/PCFV/pdf/Uganda_baseline.pdf.

[6] Mbandi AM, Böhnke JR, Schwela D, Vallack H, Ashmore MR, Emberson L. 2019. Estimating on-road vehicle fuel economy in Africa: a case study based on an urban transport survey in Nairobi, Kenya. Energies 12:1177.

[7] WHO 2002 : Reducing ridk promoting health life. Report 150p.

[8] Todd Alexander Litman 2009: Transportation Cost and Benefit Analysis Techniques, Estimates and Implications. 20p.

[9] Florent Grelier 2018: CO2 emission from cars: the

fact. 53p.
[10] SP/CNDD 2018 : Rapport de la Troisième Communication National sur le changement climatique. 45p.
[11] Thiombiano S.T; WEISMAN N; et al 2011: Adaptation de l'outil exact et évaluation de l'empreinte carbone de la filière anacarde au Burkina Faso. 4p.
[12] MEEVCC 2017 : Rapport final Inventaire Forestier National(IFN2). 74p.

BILINGUAL PUBLISHING CO.
Pioneer of Global Academics Since 1984

Journal of Atmospheric Science Research
https://ojs.bilpublishing.com/index.php/jasr

ARTICLE

Processing of Rainfall Time Series Data in the State of Rio de Janeiro

Givanildo de Gois[1] José Francisco de Oliveira-Júnior[2*]

1. Federal University of Rondônia Foundation (UNIR), Porto Velho, Rondônia, 76801-059, Brazil
2. Applied Meteorology and Environment Laboratory (LAMMA), Institute of Atmospheric Sciences (ICAT), Federal University of Alagoas (UFAL), Maceió, Alagoas, 57072-900, Brazil

ARTICLE INFO

Article history
Received: 20 August 2021
Accepted: 11 October 2021
Published: 20 October 2021

Keywords:
Data validation
Parametric tests
Cluster analysis

ABSTRACT

The goal was to perform the filling, consistency and processing of the rainfall time series data from 1943 to 2013 in five regions of the state. Data were obtained from several sources (ANA, CPRM, INMET, SERLA and LIGHT), totaling 23 stations. The time series (raw data) showed failures that were filled with data from TRMM satellite via 3B43 product, and with the climatological normal from INMET. The 3B43 product was used from 1998 to 2013 and the climatological normal over the 1947-1997 period. Data were submitted to descriptive and exploratory analysis, parametric tests (Shapiro-Wilks and Bartlett), cluster analysis (CA), and data processing (Box Cox) in the 23 stations. Descriptive analysis of the raw data consistency showed a probability of occurrence above 75% (high time variability). Through the CA, two homogeneous rainfall groups (G1 and G2) were defined. The group G1 and G2 represent 77.01% and 22.99% of the rainfall occurring in SRJ, respectively. Box Cox Processing was effective in stabilizing the normality of the residuals and homogeneity of variance of the monthly rainfall time series of the five regions of the state. Data from 3B43 product and the climatological normal can be used as an alternative source of quality data for gap filling.

1. Introduction

Rainfall is the climatic variable with high space-time variability; it can cause significant damage to society, and affect many human activities around the world [1,2]. Rainfall interferes with several socials productive sectors: such as use and power generation, tourism, agriculture, industrial production, building, aviation, and population's health problems, among others [1,3-5].

State of Rio de Janeiro (SRJ) has a high annual rainfall rate and a complex topography [6]. However, it has a heterogeneous rainfall spatial distribution, because of the interaction with the topography with coastal environment and weather systems that influence this heterogeneity [7]. Most of the studies on the rainfall in SRJ have been restricted to its time variability. There are few analyses that approach rainfall time trends without identifying the main weather systems [8,9]. The main weather systems that operate in the SRJ range from synoptic scale to site, and are classified as producers and inhibitors of rainfall. These include: Frontal Systems (FS), Mesoscale Convective Systems (MCS),

*Corresponding Author:
José Francisco de Oliveira-Júnior,
Applied Meteorology and Environment Laboratory (LAMMA), Institute of Atmospheric Sciences (ICAT), Federal University of Alagoas (UFAL), Maceió, Alagoas, 57072-900, Brazil;
Email: jose.junior@icat.ufal.br

DOI: https://doi.org/10.30564/jasr.v4i4.3603

South Atlantic Convergence Zone (SACZ), South Atlantic Subtropical High (SASH), Atmospheric Blocking (AB), wind systems (valley/ mountain, lake, bay and marine/ terrestrial), Instability Lines (IL), Mesoscale Convective Complexes (MCC), orographic rainfall, convective storms, and others [4,7-12].

These systems cause varying intensities of rainfall, depending on the location and topography of the region, or inhibit or cause strong droughts and dry spells in SRJ [4,13]. The presence of the Maciços de Pedra Branca, Tijuca and Gericinó, which comprises the Metropolitana region of Rio de Janeiro (MRJR), together with *Serra da Mantiqueira* (SW) and *Serra do Mar* (coastal) provides a barrier to air displacement at low levels of the atmosphere. This presence result in changes in the flow structure and in the weather conditions from the site and/or adjacent regions, together with Bays de Sepetiba and Guanabara, which dramatically interferes in rainfall patterns [14,15]. Seasonal and annual patterns of weather systems that operate in the SRJ may be influenced by climate variability modes, such as El Niño-Southern Oscillation (ENSO) and the Pacific Decadal Oscillation (PDO) [11,16].

SRJ has an irrigated area of 36 thousand hectares, which is small compared to other states of the Southeast region. Although the SRJ does not stand out in the Brazilian agricultural scenario, there was an increase in irrigated agricultural production, especially in regard to the fruit growing in the Norte Fluminense and Nordeste Fluminense regions [13]. Therefore, it is necessary to identify time (seasonal, interannual and decadal) and spatial (regional and large scale) patterns to subsidize activities in the agricultural and forest areas in SRJ [7,16].

To understand the rainfall patterns in a region previous knowledge is needed of the several factors that affect, for example, physiographic or dynamic, but all acting simultaneously in SRJ [7,9]. However, studies conducted over the last decades in SRJ [9,17-20] did not identify the producers and inhibitors of rainfall systems. Followed by the action of climate variability modes, as well as a treatment involving the rainfall time series of the Government regions, which were restricted to short time series with gaps.

There are few studies based on a careful analysis of rainfall time series in SRJ, most of them focusing on the gap filling and consistency of the time series. Therefore, the goal is to perform the filling, consistency and processing of the rainfall time series data from 1943 to 2013 in five government regions of the state of Rio de Janeiro by the application of descriptive and exploratory analysis, parametric tests, cluster analysis and the data processing technique.

2. Materials and Methods

2.1 Study Area

SRJ is located in Southeastern Brazil, between the latitudes 20º 45' 54 and 23º 21' 57" S and the longitudes 40º 57' 59" and 44º 53' 18" W, with an area of e 43,696,054 km². It borders to the northeast (NE) with the Espírito Santo, north and northwest (N-NW) with Minas Gerais, southwest (SW) with São Paulo and with the Atlantic Ocean to south and east (S-E). It has extensive coastline, with about 635 km long, is bathed by the Atlantic Ocean.

Currently, the SRJ is geopolitically divided into 92 municipalities [21], inserted in eight Government regions: *Metropolitana*, *Noroeste Fluminense*, *Norte Fluminense*, *Baixadas Litorâneas*, *Serrana*, *Centro-Sul Fluminense*, *Médio Paraíba* and *Costa Verde* (Figure 1). According to [22] the SRJ has a landscape with high cliffs, to sea and in the interior; hills; hills and valleys; with varied rock formations in bays with different forms of encounter between the sea and the coast; natural tropical forests followed by large areas of the plateau, which stretches to the west of the state. It stands out among the remaining the peak of Agulhas Negras with altitude of 2,787 m, in the Serra da Mantiqueira region. Serra da Mantiqueira is an important transition area of the Southeast region directed to the valley of the Paraíba do Sul River, which has the lowest height of 250 m, crossing the States of São Paulo, Rio de Janeiro and Minas Gerais.

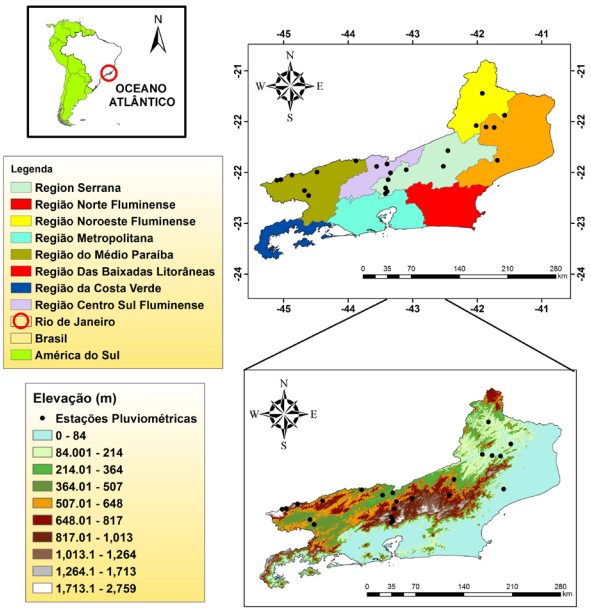

Figure 1. Location of the 23 stations distributed in five Government regions (Norte Fluminense, Noroeste Fluminense, Serrana, Centro Sul Fluminense and Médio Paraíba) of the State of Rio de Janeiro (SRJ).

2.2 Time Series of Rainfall Data 1943-2013

We used rainfall data (mm) from montlhy time series (1943 to2013) of 23 stations, being divided into: pluviometric and automatic and conventional meteorological distributed in five Government regions (*Noroeste Fluminense*, *Norte Fluminense*, *Serrana*, *Centro-Sul Fluminense* and *Médio Paraíba*) of the SRJ - (Table 1). Series was composed by data from ANA (National Water Agency), CPRM (Mineral Resources Research Company), INMET (National Institute of Meteorology), SERLA (State Superintendence of Rivers and Lakes Foundation) and LIGHT (Light Electricity Services S/A). The regions *Baixadas Litorâneas*, *Costa Verde* and *Metropolitana* did not show stations with series from 71 years and, therefore, not entered the study.

Table 1. Identification of the 23 stations distributed in five Government regions (Norte Fluminense, Noroeste Fluminense, Serrana, Centro Sul Fluminense and Médio Paraíba) of the State of Rio de Janeiro (SRJ).

N	Stations	Lat (°)	Long (°)	Altitude (m)
1	São Fidelis	-21.65	-41.75	10.00
2	Cardoso Moreira	-21.49	-41.61	20.00
3	Dois Rios	-21.64	-41.86	50.00
4	Macabuzinho	-22.08	-41.71	19.00
5	Itaperuna	-21.21	-41.91	110.00
6	Três Irmãos	-21.63	-41.99	42.00
7	Aldeia	-21.95	-42.36	376.00
8	Bom Jardim	-22.16	-42.42	530.00
9	Areal	-22.24	-43.10	450.00
10	Moura Brasil	-22.13	-43.15	270.00
11	Paraíba do Sul	-22.16	-43.29	300.00
12	Fazenda Sobradinho	-22.20	-42.90	650.00
13	Itamarati	-22.49	-43.15	1025.00
14	Pedro do Rio	-22.33	-43.14	645.00
15	Petrópolis	-22.51	-43.17	890.00
16	Rio da Cidade	-22.44	-43.17	704.00
17	Barra Mansa	-22.54	-44.18	376.00
18	Fazenda Agulhas Negras	-22.34	-44.59	1460.00
19	Ponte do Souza	-22.27	-44.39	950.00
20	Ribeirão de São Joaquim	-22.47	-44.23	620.00
21	Visconde de Mauá	-22.33	-44.54	1030.00
22	Manuel Duarte	-22.09	-43.56	396.00
23	Santa Isabel do Rio Preto	-22.23	-44.06	544.00

2.3 Gap Filling of Monthly Rainfall Time Series 1943-2013

Monthly rainfall time series that showed gaps were filled with data from TRMM (Tropical Rainfall Measuring Mission) satellite via 3B43 product and the normal climatological coming from INMET (Instituto Nacional de Meteorologia). The 3B43 product was used during the period from 1998 to 2013 and the normal climatological from INMET during 1947 to 1997. The 3B43 product was obtained in NetCDF format at the site: www.mirador.gsfc.nasa.gov/collections/TRMM_3B43_007.shtml. The product provides data with spatial from about 30 km and monthly time resolution.

The 3B43 product was converted into ArcGIS software version 10.1®. Conversion of data, originally in $mm.h^{-1}$ to accumulated monthly ($mm.monthly^{-1}$)-[4]. Selecting the TRMM points was made based on proximity of the stations within the study area. In ArcGIS software version 10.1 was used the ArcToolbox-Multidimension Tools, and the conversion tools Make NetCDF Raster Layer and Make NetCDF Table View for the procedure.

2.4 Consistency and Processing of the Rainfall Temporal Series Data 1943-2013

After the gap filling from the data, a raw time series data was built and, at lastly, we performed an exploratory and descriptive data analysis with the assistance of R software version 3.1.1 [23]. In the descriptive analysis we calculated the mean, median, maximum values, total amplitude, the lower and upper limits, the coefficients of variation (CV, %), asymmetry and kurtosis (K), standard deviation (S), lowest (LQ) and upper (UQ) quartile and interquartile amplitude (IQA). Exploratory analysis was based on boxplot and consists in identifying the outliers, which are values that are three times beyond the boxplot interquartile amplitude.

Shapiro-Wilk (*SW*) and Bartlett (*B*) tests were applied, at 0.05 probability level, for the 23 stations for testing the normality of the residues and homogeneity of data variance. SW test is used when the sample size to be tested is lower than 2,000 observations [24]. If there is no normality of the residues and homogeneity of raw data variance, the variance of the series should be stabilized before any procedure.

SW test was applied to the rainfall time series according to a normal probability distribution. It consists of the ratio from two different variance estimators. The estimator in the numerator based on a linear combination of amounts related to statistics of order from the normal distribution. The estimator in the denominator was obtained in a conventional way.

Statistic from *SW* test, *W*, is defined by Equation 1, given by:

$$W = \frac{\left[\sum_{i=1}^{k} a_{n-i+1}\left(y_{n-i+1} - y_i\right)\right]^2}{\sum_{i=1}^{n}\left(y_i - \bar{y}\right)^2} = \frac{\left[\sum_{i=1}^{k} a_i\, y_{(i)}\right]^2}{\sum_{i=1}^{n}\left(y_i - \bar{y}\right)^2} \quad (1)$$

Wherein, i = 1, 2,....n, is the sample size; y_i= Sample measurement value under analysis ordered from lowest to highest for the value ; $\bar{y}$ = mean value of measuring; *ai* = coefficient generated from the middle, variance and covariance of statistical order from a sample with n size and a normal distribution.

Wherein *X* is a feature of study, we formulate the hypothesis:

H_0: Rainfall data from the stations show residues with normal distribution (Gaussian);

H_1: Rainfall data from the stations do not show residues with normal distribution (Gaussian).

The conditions so that the data of the stations are distributed according to a normal distribution at probability level α were that:

For $W_{cal} \leq W_{tab}$ we rejected H_0 for P-value $\alpha < 0.05$;

For $W_{cal} \geq W_{tab}$ we accept H_0 for P-value $\alpha > 0.05$.

[25] test proposed by [26], was employed to verify the assumption that *K* samples from a population shows equal variances, i.e., homogeneity of variance. Statistic from Bartlett's test, *B0* is determined by the following equations:

$$N = \sum_{j=1}^{n} n_j \quad (2)$$

$$S_i^2 = \sum_{j=1}^{n_i} \frac{\left(y_j - \overline{y_i}\right)^2}{n_i - 1} \quad (3)$$

$$S_p^2 = \frac{1}{N-k}\sum_{i=1}^{k}\left(n_i - 1\right)S_i^2 \quad (4)$$

$$q = \left(N-k\right)\mathrm{h}\ S_p^2 - \sum_{i=1}^{k}\left[\left(n_i - 1\right)\mathrm{h}\ S_i^2\right] \quad (5)$$

$$c = 1 + \frac{1}{3\left(k-1\right)}\left(\sum_{i=1}^{n}\frac{1}{n_i - 1} - \frac{1}{N-k}\right) \quad (6)$$

Wherein B_0 is defined as:

$$B_0 = \frac{q}{c} \quad (7)$$

B_0 on the hypothesis $H_0 \approx \chi^2_{k-1}$

Wherein, N = number of observations, *ni* and k = number of observations within groups, S_i^2 = sample variance, S_p^2 = population variance, q= coefficient of numerator, c = coefficient of denominator, χ^2_{k-1} = chi-square distribution , a= significance level and B_0 = statistic from Bartlett's test.

Wherein *X* is a feature of study, we formulate the following hypotheses:

H_0: Rainfall data from the stations show homogeneous variances.

H_1: Rainfall data from the stations do not show homogeneous variances.

The conditions so that the data from the statins show homogeneity or heterogeneity of variances at probability level α were that:

$B_0 \geq \chi^2_{(1-\alpha,k-1)}$ we reject H_0 for P-value α < 0.05;

$B_0 \leq \chi^2_{(1-\alpha,k-1)}$ we accept H_0 for P-value α > 0.05.

is common applying a processing to the data set. Thus, in this situation was used the [27] processing. The method consists on estimating multiple values for lambda parameter (λ). In the study the quadratic processing was used in the raw time series, given by Equation 8:

$$y(\lambda) = \frac{\left(x^{\lambda} - 1\right)}{\lambda} \qquad \lambda \neq 0 \quad (8)$$

wherein, x = raw data and λ= lambda.

Later it was performed the cluster analysis of time series data processed by software environment R version 3.1.1 [23]. Thus, we determined the respective numbers of groups and the dendrogram. Number of groups adopted and stratification of stations was based on Ward's hierarchical agglomerative method [28] through the dissimilarity measure from Euclidean distance [29,30].

Euclidean distance is given by:

$$d_E = \sqrt{\sum_{j=1}^{p}(x_j - x_k)^2} \quad (9)$$

wherein, *dE* = Euclidean distance; x_{ij} and x_{kj} = quantitative parameters *j* from *p* and *k* individuals, respectively.

On [29] the distance between two clusters is the sum of the squares among the two clusters made on all variables. In this method, we minimize the dissimilarity or minimize the total of the sums of squares within groups, i.e., occurs by the homogeneity within each group and heterogeneity out of each group [31].

$$W = \sum_{i=1}^{n} x_i^{\,2} - \frac{1}{n}\left(\sum x_i\right)^2 \quad (10)$$

wherein, W = within group homogeneity and heterogeneity by the sum the squares of the deviations; n = number of analyzed values; xi = i-th element of the cluster.

According to [32], the method reveals itself as one of the most suitable on the cluster analysis, wherein the time series rainfall data are arranged in array form $P_{(n\,x\,p)}$ where P_{ij} represents the i-th variable value (site) of the j-th individual (monthly). Each row vector represents the rainfall within the year and each column vector represents the season.

After the cluster analysis, we separate between the five study regions the stations that showed better performance according to the SW and B parametric tests, and were subsequently made to analyze the position and dispersion measures, in order to verify how the empirical distribution approaches from the normal, which is statistically evidenced by non-parametric test.

Considering that the position and dispersion measurements are influenced by the presence of discrepant values (outliers) or extreme, an exploratory data analysis was performed to detect the presence of outliers using descriptive statistics previously cited, followed by the boxplot and normal probability graph. Again, we used the software R version 3.1.1 [23], for calculating the all indexes and statistical graphs.

After applying the Box Cox processing, the stations that had better performance according to *SW* and *B* test were separated. Subsequently, the analysis of the position and dispersion measurements was performed in order to verify how the empirical distribution approaches from the normal, which is evidenced statistically by non-parametric tests.

3. Results

3.1 Descriptive Statistics and Exploratory Data Analysis of Raw Rainfall Data

Time series monthly rainfall in the State Government regions with a probability of occurrence above 75% showed high temporal variability, mainly in the maximum parameter ranging among 397.00 to 1277.90 mm, followed by total amplitudes in the same proportion (Tables 2 to 6). Sample CV for all existing stations in five Government regions was higher than 70%. This indicates a significant dispersion and heterogeneity of raw rainfall data, allowing highlight important features in the Government regions, regarding to producers and inhibitors of rainfall systems, in the SRJ. However, *Moura Brasil* (217.66%) and *Paraíba do Sul* (105.40%,) stations stood out over the others with the highest sample CV, respectively (Table 4).

In the analysis of the lower and upper limits as outlier's delimiters, we observed values higher than the 75th percentile from the time series in all seasons outside of this range, confirmed by standard deviation and the IQA (Figure 2). The highest standard deviations about the mean were: in Norte Fluminense region, at *São Fidelis* (80.03 mm), *Dois Rios* (81.04) and *Macabuzinho* (94.77) regions; in *Noroeste Fluminense*, at *Itaperuna* (90.95 mm) and *Três Irmãos* (88.45 mm); in *Centro-Sul Fluminense*, at Areal (103.78 mm) and *Paraíba do Sul* (106.54 mm). In *Serrana* region, at the *Aldeia* (102.42 mm), *Bom Jardim* (112.37 mm) and *Fazenda Sobradinho* (109.44 mm) stations; in the *Médio Paraíba* regions, at the *Barra Mansa* (99.63 mm) and *Manuel Duarte* (106.73 mm) stations.

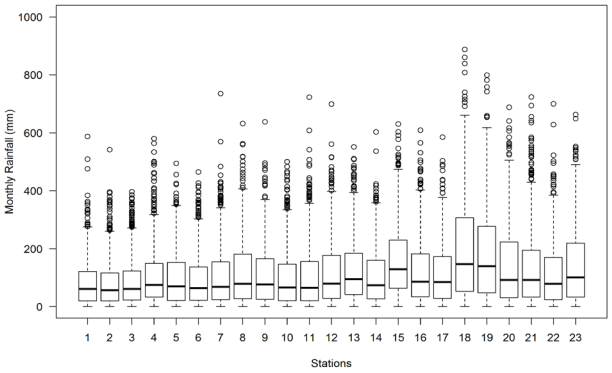

Figure 2. Boxplot of the monthly rainfall time series of raw data from Norte Fluminense, Noroeste Fluminense, Serrana, Centro Sul Fluminense and Médio Paraíba regions of the State of Rio de Janeiro (SRJ).

Through the boxplot and descriptive analysis of the monthly raw rainfall data from the regions of SRJ we verified a similarity of the median parameter in all seasons. The values were lower than the means, being the means influenced by high rainfall values (outliers), which indicates that distributions for the five regions of the state are skewed (asymmetric) to the right (Figure 3). However, we observed values equal to median (61.15 mm) at *São Fidelis* and *Dois Rios* stations (Table 2). *Macabuzinho's* station recorded the highest value for mean (102.72 mm) and median (75.30 mm), respectively. *Nordeste Fluminense, Centro-Sul Fluminense, Serrana* and *Médio Paraíba* regions followed the same behavior towards higher values for the mean and median, in the respective, *Itaperuna, Areal, Petrópolis* and *Fazenda Agulhas Negras* stations (Tables 2 to 6).

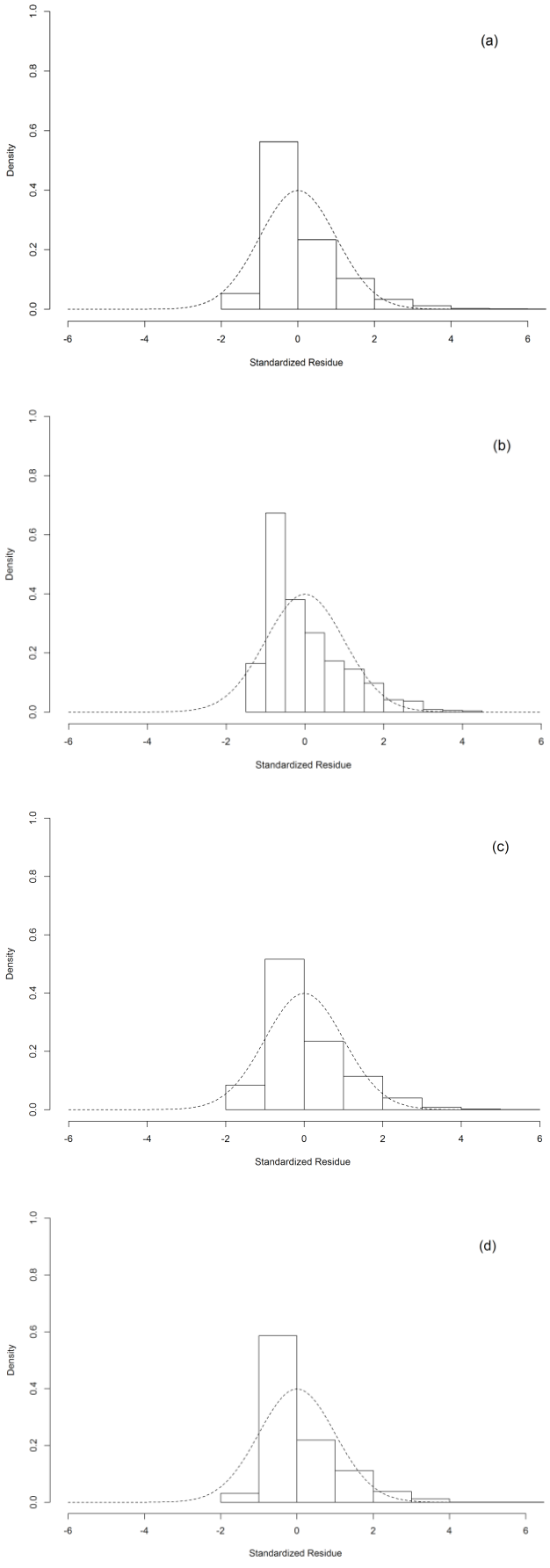

Figure 3. Histograms of the monthly rainfall series of raw data from Norte Fluminense (a), Noroeste Fluminense (b), Serrana (c), Centro Sul Fluminense (d) and Médio Paraíba (e) regions of the State of Rio de Janeiro (SRJ).

Positive asymmetry coefficients (*K*) ranged from 1.16 to 3.60 for the five regions from the State Government. The *K* coefficient characterizes how the data distribution deviates from symmetrical condition. In this case, the tail on the right is more elongated than the tail to the left to middle > 0, which indicates the occurrence of high values with a low frequency - (Figure 3). The *K* coefficient in the *North* region for the *São Fidelis* and *Macabuzinho* stations show that the form of the data distribution is leptokurtic ($K > 3$, more tapered curve), and for the *Cardoso Moreira* and *Dois Rios* stations is platykurtic ($K < 3$, flatter curve). Although the distribution form for the *Cardoso Moreira* station is close to mesokurtic form ($K = 3$, curve neither too flattened nor too tapered), feature of normal distribution (Table 2).

In *Nordeste* region, there is a predominance of a flatter frequency curve ($K < 3$), whose raw data distribution form for the stations from *Itaperuna* and *Dois Rios* is platykurtic (Table 3). The results obtained in *Serrana* region, for the *K* coefficient show that the level of flattening of the frequency curve for all seven stations were platykurtic. However, *Itamarati* station (2.97) obtained *K* coefficient close to 3, where the distribution may be considered in mesokurtic form (Table 5).

The *K* coefficients for the *Centro-Sul* region suggest that the degree of flattening of the frequency curves of the *Areal, Paraíba do Sul* and *Moura Brasil* stations are platykurtic and leptokurtic respectively. However, we observe that in Paraíba station, the *K* coefficient is close to 3, providing mesokurtic distribution (Table 4). The K coefficient for the Médio Paraíba region indicates the platykurtic predominance for *Barra Mansa, Fazenda Agulhas Negras, Ponte do Souza, Visconde de Mauá* and *Manuel Duarte* stations, and leptokurtic for *Ribeirão de São Joaquim* and *Santa Isabel do Rio Preto* (Table 6).

Table 2. Descriptive statistics of the monthly rainfall data (mm) in Norte Fluminense region, State of Rio de Janeiro (SRJ).

Stations	Mean (mm)	Median (mm)	Value	Total Amplitude (mm)	Limit	
			Maximum (mm)		Lower (mm)	Upper (mm)
São Fidelis	82.49	61.15	587.80	587.80	-134.51	275.78
Cardoso Moreira	79.78	56.44	542.00	542.00	-125.20	270.36
Dois Rios	85.16	61.15	397.00	397.00	-126.37	276.94
Macabuzinho	102.72	75.30	580.20	580.20	-140.35	302.71

Stations	Coefficient			Sample Standard Deviation (mm)	Quartile		Interquartile amplitude (mm)
	Sample variation (%)	Asymmetry	Kurtosis (K)		Lower (mm)	Upper (mm)	
São Fidelis	97.03	1.54	3.60	80.03	19.35	121.92	102.57
Cardoso Moreira	97.36	1.51	2.82	77.67	19.82	116.50	96.68
Dois Rios	95.17	1.36	1.54	81.04	23.30	123.08	99.78
Macabuzinho	92.26	1.65	3.48	94.77	33.17	148.85	115.68

Table 3. Descriptive statistics for the monthly rainfall data (mm) in *Noroeste* region, State of Rio de Janeiro.

Stations	Mean (mm)	Median (mm)	Value	Total Amplitude (mm)	Limit	
			Maximum (mm)		Lower (mm)	Upper (mm)
Itaperuna	96.01	69.75	494.80	494.80	-176.36	306.43
Três Irmãos	91.66	63.70	464.90	464.90	-149.73	290.01

Stations	Coefficient			Sample standard deviation (mm)	Quartile		Interquartile Amplitude (mm)
	Sample variation (%)	Asymmetry	Kurtosis (K)		Lower (mm)	Upper (mm)	
Itaperuna	94.73	1.16	0.95	90.95	21.00	152.57	131.57
Três Irmãos	96.50	1.27	1.22	88.45	21.80	136.15	114.35

Table 4. Descriptive statistics for the monthly rainfall data (mm) in *Centro Sul* region, State of Rio de Janeiro.

Stations	Mean (mm)	Median (mm)	Value	Total Amplitude (mm)	Limit	
			Maximum (mm)		Lower (mm)	Upper (mm)
Areal	109.04	76.20	638.30	638.30	-183.55	319.11
Moura Brasil	96.56	65.88	500.00	500.00	-169.43	300.11
Paraíba do Sul	101.08	64.55	723.00	723.00	-183.10	309.26

Stations	Coefficient			Sample standard deviation (mm)	Quartile		Interquartile Amplitude (mm)
	Sample variation (%)	Asymmetry	Kurtosis (K)		Lower (mm)	Upper (mm)	
Areal	95.17	1.25	1.42	103.78	25.73	165.25	139.52
Moura Brasil	217.66	2.87	6.55	39.20	19.98	146.25	126.27
Paraíba do Sul	105.40	1.56	2.85	106.54	20.00	155.40	135.40

Table 5. Descriptive statistics for the monthly rainfall data (mm) in *Serrana* region, State of Rio de Janeiro.

Stations	Mean (mm)	Median (mm)	Value	Total Amplitude (mm)	Limit	
			Maximum (mm)		Lower (mm)	Upper (mm)
Aldeia	102.59	68.56	735.60	735.60	-171.58	307.71
Bom Jardim	116.20	78.80	632.00	632.00	-201.10	334.26
Fazenda Sobradinho	114.33	79.50	699.00	699.00	-195.05	330.86
Itamarati	126.20	95.30	551.20	551.20	-171.53	337.96
Pedro do Rio	104.70	73.50	603.50	603.50	-173.55	314.06
Petrópolis	158.50	129.00	630.20	630.20	-186.40	383.46
Rio da Cidade	121.04	85.92	609.40	609.40	-187.63	336.06

Stations	Coefficient			Sample standard deviation (mm)	Quartile		Interquartile Amplitude (mm)
	Sample variation (%)	Asymmetry	Kurtosis (K)		Lower (mm)	Upper (mm)	
Aldeia	99.83	1.43	2.50	102.42	23.68	153.85	130.17
Bom Jardim	96.73	1.26	1.31	112.37	27.80	180.40	152.60
Fazenda Sobradinho	95.72	1.30	1.70	109.44	28.18	177.00	148.82
Itamarati	84.76	1.12	2.97	7.90	41.85	184.10	142.25
Pedro do Rio	93.88	1.16	1.11	98.32	26.70	160.20	133.50
Petrópolis	77.30	3.52	1.98	9.06	63.20	229.60	166.40
Rio da Cidade	90.83	1.18	1.08	8.12	34.27	182.20	147.93

Table 6. Descriptive statistics for the monthly rainfall data (mm) in *Médio Paraíba* region, State of Rio de Janeiro.

Stations	Mean (mm)	Median (mm)	Value	Total Amplitude (mm)	Limit	
			Maximum (mm)		Lower (mm)	Upper (mm)
Barra Mansa	110.10	84.90	585.60	585.60	-186.78	326.06
Fazenda Agulhas Negras	195.92	147.05	888.20	888.20	-328.72	460.79
Ponte do Souza	175.82	139.40	799.50	799.50	-295.63	430.56
Ribeirão de São Joaquim	141.76	91.85	1243.00	1243.00	-256.91	376.43
Visconde de Mauá	133.50	91.80	724.00	724.00	-208.15	347.46
Manuel Duarte	111.30	78.40	700.00	700.00	-195.33	323.66
Santa Isabel do Rio Preto	141.15	101.09	1277.90	1277.90	-247.05	372.81

Stations	Coefficient			Sample standard deviation (mm)	Quartile		Interquartile Amplitude (mm)
	Sample variation (%)	Asymmetry	Kurtosis (K)		Lower (mm)	Upper (mm)	
Barra Mansa	90.50	1.12	1.12	99.63	28.61	172.20	143.59
Fazenda Agulhas Negras	86.81	3.60	1.79	12.57	52.67	306.93	254.26
Ponte do Souza	85.81	3.58	2.17	11.15	47.77	276.70	228.93
Ribeirão de São Joaquim	99.79	1.57	4.55	10.45	30.78	222.57	191.79
Visconde de Mauá	99.03	1.43	1.87	9.77	32.90	193.60	160.70
Manuel Duarte	95.90	1.29	2.01	106.73	23.75	169.80	146.05
Santa Isabel do Rio Preto	95.54	1.60	5.92	9.97	32.55	218.95	186.40

3.2 Processing of Time Series Rainfall Data

Values from *SW* and *B* tests and Q-Q Plt Normal probabilistic graphs (Figure 4) applied to the raw rainfall data series considering 0.05 probability level, indicates the non-normality of residues and heterogeneity of variances in all seasons, being, therefore, verified the non-stability of data variance (Table 7).

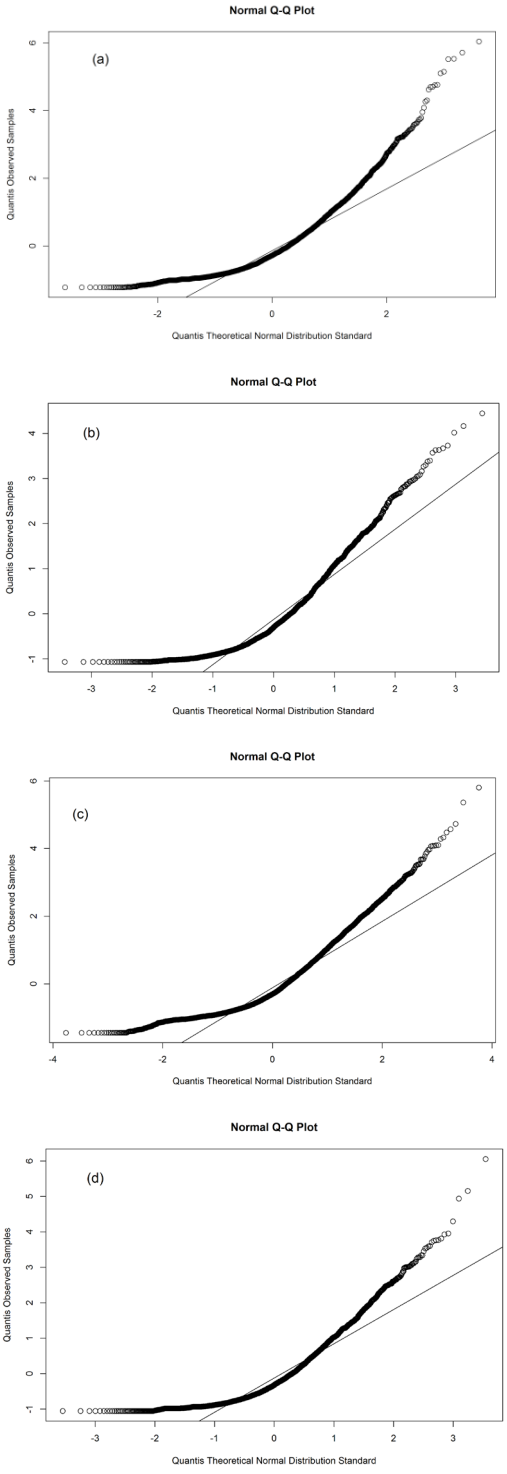

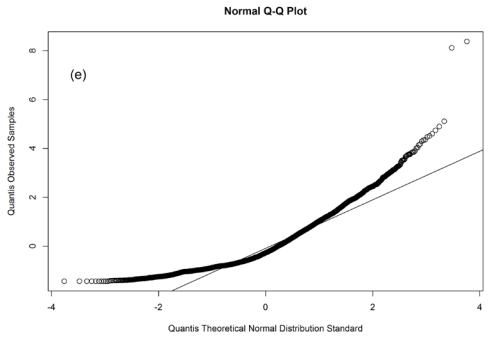

Figure 4. Quartile-Quantile Plot graphs from monthly rainfall series of raw data from Norte Fluminense (a), Noroeste Fluminense (b), Serrana (c), Centro Sul Fluminense (d) and Médio Paraíba (e) regions of the State of Rio de Janeiro (SRJ).

From this, it was necessary to stabilize the variance from the time series by applying the Box-Cox processing, where the λ values ranged from 0.33 to 0.44, (Table 7). Processed data from the *Norte Fluminense, Nordeste Fluminense, Centro-Sul Fluminense, Serrana* and *Médio Paraíba* regions recorded the highest p-value ($\alpha > 0.05$) for SW and B tests, mainly in Dois Rios (0.05 and 0.159), *Macabuzinho* (0.06 and 0.09), *Itaperuna* (0.37 and 0.23), *Três Irmãos* (0.11 and 0.06), *Paraíba do Sul* (0.28 and 0.27), *Bom Jardim* (0.14 and 0.32) and *Fazenda Sobradinho* (0.43 and 0.27) stations. This shows that after processing of rainfall data there was adjustment to normal distribution (Figure 5 and Table 7).

However, *Médio Paraíba* and *Serrana* regions stood out among the five regions of the state, such as those that record the largest number of stations with the lowest values for p-value ($\alpha < 5\%$) in the stations: *Fazenda Agulhas Negras* (0.01 and 0.001), *Ribeirão de São Joaquim* (0.01 and 0.001), *Manuel Duarte* (0.03 and 0.001), *Santa Isabel do Rio Preto* (0.00 and 0.001) and *Petrópolis* (0.00 and 0.001). Some of the stations from *Norte* and *Centro-Sul Fluminense* regions did not show adjustment of the residues to normal distribution, as *Cardoso Moreira* (0.03 and 0.010) and *Areal* (0.02 and 0.020).

Based on cluster analysis technique (CA) were set two rainfall homogeneous groups (G_1 and G_2) for the 23 stations (Figure 6). The stations belonging to G_1 are located on the slope of the Serra do Mar directed to the interior (20 stations) and the others (3 stations) on the slope of the Serra do Mar directed to the coastal environment (Figure 1). The stations belonging to the group G_2, *Fazenda Agulhas Negras* and *Ponte do Souza* (Médio Paraíba) and *Petropólis* (Serrana) show elevations above 850 m (Table 1). It is important to note the difference in the rainfall regime between the G_1 and G_2, where the first stands out for

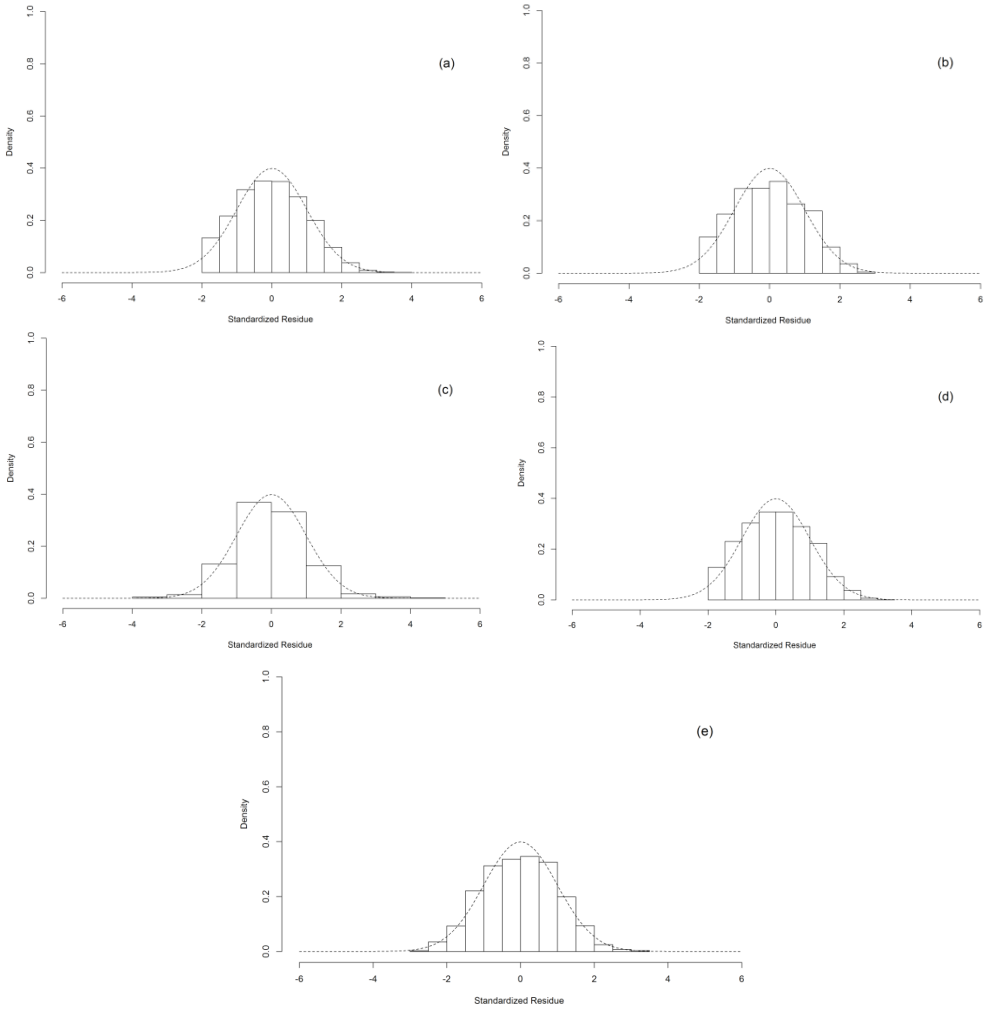

Figure 5. Histograms of the processed data of monthly rainfall series from Norte Fluminense (a), Noroeste Fluminense (b), Serrana (c), Centro Sul Fluminense (d) and Médio Paraíba (e) regions of the State of Rio de Janeiro (SRJ).

its largest annual accumulated 1164.95 mm.year^{-1} compared to group G_2 with an accumulated rainfall of 347.86 mm.year^{-1}, representing, respectively 77.01% and 22.99% of the rainfall in five SRJ Government regions (Table 8).

Box Cox proceeding was effective as processing of the time-series data in accordance with the *SW* and *B* tests, showing the non-violation of normality and homogeneity of variance premises. The best performance based on the CA technique was observed in the group G_1.

Results concerning the descriptive and exploratory analysis of the processed data showed that the *Box-Cox* processing stabilized the data variance (outliers) in all 23 stations. It is important to note the similarity regarding the mean behavior that approached the median values in all regions of the state, compared to the raw data from the time series, previously discussed time series. The distribution form of the monthly rainfall time series for the five Government regions approaches a symmetrical distribution (mean and median practically equal), proven by low asymmetry coefficient values (0.02 to 0.22), indicating that the means of station of the groups G_1 and $G_2$are close to the median (Table 8). The results of the *K* coefficients from the stations belonging to the groups G_1 and G_2reveal that the flattening level of the frequency curve for all stations are platykurtic ($K < 3$), as shown in Figure 5 and Table 8. The obtained results were corroborated by the values from descriptive analysis, which indicates a low temporal variability of the data, with maximum values ranging from 24.10 mm to 31.78 mm in G_1 followed by total amplitudes in the same ratio and upper and lower limits on the order of -4.69 mm to 34.37 mm.

CV analysis for the groups G_1 and G_2 shows that all stations had values above 30%, indicating high dispersion of rainfall data for the whole study area. This situation is corroborated by higher standard deviation and upper IQA, which indicate a high data variability level around the

Table 7. Normality and homogeneity of variance test for the raw and processed rainfall data of the State of Rio de Janeiro (SRJ).

Government regions	Stations	Raw data		Processed data		lambda (λ)
		Shapiro	Bartllet	Shapiro	Bartllet	
		p-value	p-value	p-value	p-value	
NORTE	São Fidelis	2.48×10^{-7}	2.48×10^{-7}	0.01	0.189	0.425
	Cardoso Moreira	2.48×10^{-7}	2.48×10^{-7}	0.03	0.010	0.417
	Dois Rios	2.48×10^{-7}	2.48×10^{-7}	0.05	0.159	0.433
	Macabuzinho	2.48×10^{-7}	2.48×10^{-7}	0.06	0.092	0.401
NOROESTE	Itaperuna	2.48×10^{-7}	2.48×10^{-7}	0.37	0.233	0.432
	Três Irmãos	8.99×10^{-7}	2.48×10^{-7}	0.11	0.065	0.393
CENTRO SUL	Areal	2.48×10^{-7}	2.48×10^{-7}	0.02	0.020	0.425
	Moura Brasil	2.48×10^{-7}	2.48×10^{-7}	0.05	0.000	0.409
	Paraíba do Sul	2.48×10^{-7}	2.48×10^{-7}	0.28	0.273	0.335
SERRANA	Aldeia	2.48×10^{-7}	2.48×10^{-7}	0.02	0.141	0.385
	Bom Jardim	2.48×10^{-7}	2.48×10^{-7}	0.14	0.322	0.409
	Fazenda Sobradinho	2.48×10^{-7}	2.48×10^{-7}	0.43	0.274	0.385
	Itamarati	1.22×10^{-6}	2.48×10^{-7}	0.82	0.001	0.443
	Pedro do Rio	2.48×10^{-7}	2.48×10^{-7}	0.06	0.001	0.411
	Petrópolis	6.55×10^{-6}	2.48×10^{-7}	0.00	0.001	0.565
	Rio da Cidade	2.48×10^{-7}	2.48×10^{-7}	0.45	0.000	0.402
MÉDIO PARAÍBA	Barra Mansa	2.48×10^{-7}	2.48×10^{-7}	0.06	0.005	0.452
	Fazenda Agulhas Negras	2.48×10^{-7}	2.48×10^{-7}	0.01	0.001	0.431
	Ponte do Souza	2.48×10^{-7}	2.48×10^{-7}	0.13	0.000	0.437
	Ribeirão de São Joaquim	2.48×10^{-7}	2.48×10^{-7}	0.01	0.001	0.361
	Visconde de Mauá	2.48×10^{-7}	2.48×10^{-7}	0.49	0.000	0.352
	Manuel Duarte	2.48×10^{-7}	2.48×10^{-7}	0.03	0.001	0.326
	Santa Isabel do Rio Preto	2.48×10^{-7}	2.48×10^{-7}	0.00	0.001	0.326

mean, at *Itaperuna* (7.14 mm-11.57 mm) in G_1, *Petrópolis* (13.83 mm-19.69 mm) and *Fazenda Agulhas Negras* (8.92 mm-14.51 mm) in G_2. Comparatively, *Macabuzinho* (5.78 mm-8.31 mm), *Três Irmãos* (5.87 mm-8.91 mm) and *Paraíba do Sul* (5.23 mm-7.94 mm) stations, inserted in the group G_1 and presented the smallest variations in the sample standard deviation and IQA. However, it was observed that the *Petrópolis* station (group G_2), despite to meet the assessed premises, has a mean higher than the median, followed by higher maximum values, total amplitude (65.85 mm) and lower (-12.72 mm) and upper (66.05 mm) limits (Table 7). Thus, the distribution form of the monthly rainfall time series for *Petrópolis* station is biased to the right, and the same is influenced by high rainfall values (Figure 7).

Table 8. Summary of descriptive statistics of processed data from monthly rainfall time series (mm) by Box Cox Processing for the regions of the State of Rio de Janeiro (SRJ).

Homogeneous Groups	Stations	Mean (mm)	Median (mm)	Value		Limit	
				Maximum (mm)	Total Amplitude (mm)	Lower (mm)	Upper (mm)
G_1	Dois Rios	11.76	11.50	28.54	28.54	-7.26	30.46
G_1	Macabuzinho	11.94	11.69	29.52	29.52	-4.69	28.57
G_1	Itaperuna	12.32	12.26	31.48	31.48	-10.87	35.41
G_1	Três Irmãos	10.73	10.56	25.92	25.92	-7.21	28.41
G_1	Bom Jardim	12.60	12.22	31.78	31.78	-9.07	34.37
G_1	Paraíba do Sul	9.14	9.13	24.10	24.10	-6.62	25.14
G_2	Petrópolis	26.82	25.92	65.85	65.85	-12.72	66.05
G_2	Fazenda Agulhas Negras	17.90	17.68	40.99	40.99	-11.18	46.87

Homogeneous Groups	Stations	Coefficient			Sample standard deviation (mm)	Quartile		Interquartile Amplitude (mm)
		Sample variation (%)	Asymmetry	Kurtosis (K)		Lower (mm)	Upper (mm)	
G_1	Dois Rios	55.70	0.22	-0.56	6.55	6.88	16.32	9.43
G_1	Macabuzinho	48.37	0.22	-0.27	5.78	7.78	16.10	8.31
G_1	Itaperuna	57.78	0.13	-0.82	7.14	6.48	18.06	11.57
G_1	Três Irmãos	34.50	0.15	-0.77	5.87	6.15	15.06	8.91
G_1	Bom Jardim	55.42	0.16	-0.78	6.98	7.22	18.08	10.86
G_1	Paraíba do Sul	57.27	0.03	-0.74	5.23	5.29	13.23	7.94
G_2	Petrópolis	51.52	0.19	-0.52	13.83	16.82	36.51	19.69
G_2	Fazenda Agulhas Negras	49.79	0.08	-0.92	8.92	10.59	25.10	14.51

Rainfall (mm)	Homogeneous Groups	
	G_1	G_2
Accumulated annual	1164.95	347.86
Percentage (%) in the homogeneous groups	77.01	22.99

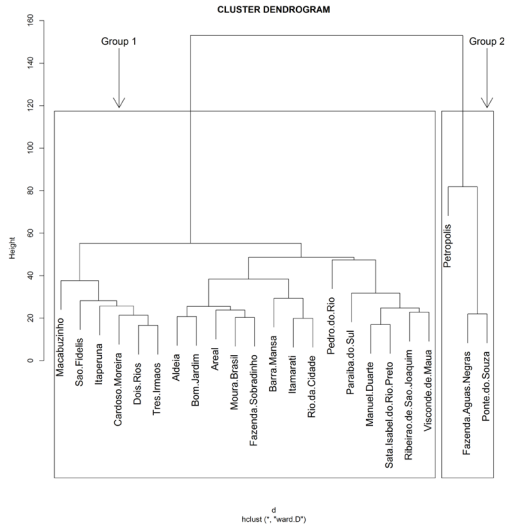

Figure 6. Dendrogram of cluster analysis of monthly rainfall time series of processed data for Norte Fluminense, Noroeste Fluminense, Serrana, Centro Sul Fluminense and Médio Paraíba regions of the State of Rio de Janeiro (SRJ).

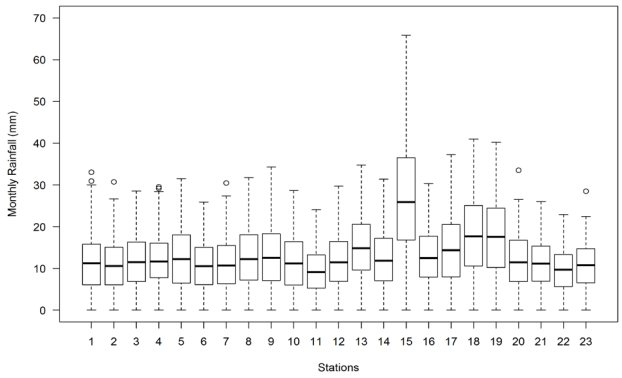

Figure 7. Boxplot of the monthly rainfall time series of the data processed by Box Cox for Norte Fluminense, Noroeste Fluminense, Serrana, Centro Sul Fluminense and Médio Paraíba regions of the State of Rio de Janeiro (SRJ).

Table 7. Normality and homogeneity of variance test for the raw and processed rainfall data of the State of Rio de Janeiro (SRJ).

Government regions	Stations	Raw data		Processed data		lambda (λ)
		Shapiro	Bartllet	Shapiro	Bartllet	
		P-value	P-value	P-value	P-value	
NORTE	São Fidelis	2.48×10^{-7}	2.48×10^{-7}	0.01	0.189	0.425
	Cardoso Moreira	2.48×10^{-7}	2.48×10^{-7}	0.03	0.010	0.417
	Dois Rios	2.48×10^{-7}	2.48×10^{-7}	0.05	0.159	0.433
	Macabuzinho	2.48×10^{-7}	2.48×10^{-7}	0.06	0.092	0.401
NOROESTE	Itaperuna	2.48×10^{-7}	2.48×10^{-7}	0.37	0.233	0.432
	Três Irmãos	8.99×10^{-7}	2.48×10^{-7}	0.11	0.065	0.393
CENTRO SUL	Areal	2.48×10^{-7}	2.48×10^{-7}	0.02	0.020	0.425
	Moura Brasil	2.48×10^{-7}	2.48×10^{-7}	0.05	0.000	0.409
	Paraíba do Sul	2.48×10^{-7}	2.48×10^{-7}	0.28	0.273	0.335
SERRANA	Aldeia	2.48×10^{-7}	2.48×10^{-7}	0.02	0.141	0.385
	Bom Jardim	2.48×10^{-7}	2.48×10^{-7}	0.14	0.322	0.409
	Fazenda Sobradinho	2.48×10^{-7}	2.48×10^{-7}	0.43	0.274	0.385
	Itamarati	1.22×10^{-6}	2.48×10^{-7}	0.82	0.001	0.443
	Pedro do Rio	2.48×10^{-7}	2.48×10^{-7}	0.06	0.001	0.411
	Petrópolis	6.55×10^{-6}	2.48×10^{-7}	0.00	0.001	0.565
	Rio da Cidade	2.48×10^{-7}	2.48×10^{-7}	0.45	0.000	0.402
MÉDIO PARAÍBA	Barra Mansa	2.48×10^{-7}	2.48×10^{-7}	0.06	0.005	0.452
	Fazenda Agulhas Negras	2.48×10^{-7}	2.48×10^{-7}	0.01	0.001	0.431
	Ponte do Souza	2.48×10^{-7}	2.48×10^{-7}	0.13	0.000	0.437
	Ribeirão de São Joaquim	2.48×10^{-7}	2.48×10^{-7}	0.01	0.001	0.361
	Visconde de Mauá	2.48×10^{-7}	2.48×10^{-7}	0.49	0.000	0.352
	Manuel Duarte	2.48×10^{-7}	2.48×10^{-7}	0.03	0.001	0.326
	Santa Isabel do Rio Preto	2.48×10^{-7}	2.48×10^{-7}	0.00	0.001	0.326

4. Discussion

The stations belonging to *Centro-Sul Fluminense*, *Serrana* and *Médio Paraíba* regions are influenced by systems ranging from local to synoptic scale, such as valley/mountain breeze circulation, the local convection, MCC, FS, SACZ, SASH and AB [7,9,12]. Displacement of synoptic systems occurs in the side from Serra do Mar directed toward the interior of the state with North-Northeast direction (N/NE). *Médio Paraíba* region is influenced by the same systems, but the displacement occurs on the side of the *Mantiqueira* directed toward Southwest-Northwest portions (SW/NW) [7,33,34].

IOR analysis also confirmed the high level of variability of raw data regarding the presence of outliers in the studied stations, being *Bom Jardim* (152.60 mm) and *Fazenda Sobradinho* (148.82 mm) those that presented the highest values. *Serrana* and *Médio Paraíba* regions showed IQA higher than the highest rainfall means, and the highest and lowest standard deviations, followed by the *Norte*, *Nordeste* and *Centro-Sul Fluminense* regions, which also showed some stations with the highest and lowest standard deviations and IQA (Tables 2 to 6).

According to [35] and [36], during winter season, there is an increased frequency of FS passages in the Southeast Brazil (SEB). However, these systems move with greater speed and find more difficultly to reach the interior of the state. Thus, the rainfall regime is limited to coast and *Serrana* and *Médio Paraíba* regions, where is located part of the state's stations [9,12]. However, stations in different regions of the state differ in relation to systems and preferred displacement as, for example, stations located at *Serrana* and *Centro-Sul Fluminense* regions, which are influenced by valley/mountain breeze circulation, local convection, FS, SACZ, SASH and AB [4,7,11]. The stations located in the *Norte* and *Nordeste Fluminense* are influenced by the same local and synoptic scale systems and, except for maritime/terrestrial breeze circulation [7,16,34]. The displacement of the systems at *Serrana* and *Centro-Sul Fluminense* regions occurs in the direction North/Northeast (N/NE) to the side of the Serra do Mar directed to the continent, while the flow for the stations from *Norte* and *Nordeste Fluminense* occurs preferably from North/Northeast/Southeast (N/NE/SE) [7].

As previously mentioned, the stations from *Norte Fluminense, Centro-Sul Fluminense, Serrana* and *Médio Paraíba*. It are highly influenced by the proximity to the coastal environment, especially the maritime/terrestrial breeze circulation which intensifies the FS, most frequently in winter, carrying moisture from the Atlantic Ocean to the continent, in addition to IL and MCC (synoptic and mesoscale) [7,20]. Stations from *Itaperuna* and *Três Irmãos* in *Nordeste Fluminense* region are away from the coast. [37] claim that the SRJ as the autumn-winter period progresses, the state's coastline starts to present the highest rainfall values.

Studies carried out by [38] with 15 normality tests using simulations with Monte Carlo method, demonstrate that the power, ease of implementation and test choice depends on many factors, including the type of distribution under alternative hypothesis, the sample size and values critics. The authors affirm that the SW test, among the used tests, provided an overall indicative of non-normality on several alternatives, symmetrical or non-symmetrical, heavy or light tails, and at lastly, on all sample sizes used. [39] compared 33 normality tests and did not mention a single efficient test compared to others in all evaluated cases. They classified tests according common features in each group, and recommend the SW among the most powerful tests for asymmetric distributions, followed by distributions which are mixtures of normal, or normal with presence of outliers when the kind of the non-normality is not known a priori. According to [40], in some situations parametric tests may disagree with the statistical decision by presenting a high sensitivity to normality violation. One of the classic examples of this sensitivity to violation is the Bartlett test for homogeneity of variance, which is seriously, affected by the non-normality, since it present a low power, and in many situations where data are not originated from a normal distribution, these tests reject the null hypothesis.

According to [7] the groups (G_1 and G_2) existing in the SRJ are formed due not only by the influence of the main synoptic systems that act in the SEB region, but mainly because of the proximity to the coastal environment and the complex topography. These local features induce to formation of orographic and convective rainfall and the rainfall regime produced by valley/mountain, lake/bay and maritime/terrestrial breeze circulation, in addition to intensify some systems, for example, IL, FS and MCC. This is due to the low frequency of outlier occurrence, or extreme values in the processed series [41].

5. Conclusions

Data from 3B43 product of the TRMM satellite together with the climatological normal from INMET can be used for gap filling and building of a time series and, especially in the study of rainfall pattern in the State of Rio de Janeiro. The descriptive analysis on the data consistency of the monthly rainfall time series data (raw) in the regions Norte Fluminense, Noroeste Fluminense, Centro-Sul Fluminense, Serrana and Médio Paraíba of

the state of Rio de Janeiro revealed that the data with a probability of occurrence above 75% show high temporal variability. Based on cluster analysis, we defined two rainfall homogeneous groups representing rainfall in the five regions of SRJ Government, respectively. Shapiro-Wilk and Bartllet tests applied to the raw data show that the data do not exhibit normality and homogeneity of variance. Box Cox processing is effective for stabilizing the homogeneity of variances and normality of the residues from monthly rainfall time series in the five regions of the State of Rio de Janeiro. Applicating the statistics tools and parametric tests are efficient in terms of data consistency from monthly rainfall time series, and on understanding of the rainfall patterns in the State of Rio de Janeiro.

Author Contributions

The first author wrote the article and made the figures. The second author reviewed the manuscript and contributed to the writing and discussion of results and conclusions.

Conflict of Interest

None.

Acknowledgments

The authors acknowledge the Agência Nacional de Águas (ANA), Companhia de Pesquisa de Recursos Minerais (CPRM), Instituto Nacional de Meteorologia (INMET), SERLA Fundação Superintendência Estadual de Rios e Lagoas and Light Serviços de Eletricidade S/A by gently give in the data for composing the rainfall time series, and the CAPES for granting Doctorate scholarship. The second author thanks Brazilian National Council for Scientific and Technological Development (CNPq) for granting the Research Productivity Fellowship level 2 (309681/2019-7).

References

[1] IPCC - Intergovernmental Panel on Climate Change (2007). Climate Change 2007: The Physical Science Basis. Summary for Policymakers Contribution of Working Group I to the Fourth Assessment Report of the Intergovernmental Panel on Climate Change, 18 pp.

[2] Tammets, T., Jaagus J. Climatology of precipitation extremes in Estonia using the method of moving precipitation totals. Theoretical and Applied Climatology, 111, 3-4, 623-639, 2013. https://doi.org/10.1007/s00704-012-0691-1.

[3] Nadarajah, S., Choi, D. Maximum daily rainfall in South Korea. Journal of Earth System Science, 116, 4, 311-320, 2007. https://doi.org/10.1007/s12040-007-0028-0.

[4] Oliveira-Júnior, J.F., Delgado, R.C., Gois, G., Lannes, A., Dias, F.O., Souza, J.C.S., Souza, M. Análise da Precipitação e sua Relação com Sistemas Meteorológicos em Seropédica, Rio de Janeiro. Floresta e Ambiente, 21, 2, 140-149, 2014. 10.4322/floram.2014.030.

[5] Westra, S., Alexaqnder, L.V., Zwiers, F.W. Global increasing trends in annual maximum daily precipitation. Journal of Climate, 26, 11, 3903-3918, 2013. https://doi.org/10.1175/JCLI-D-12-00502.1.

[6] Reboita, M.S., Gan, M. A, Rocha, R.P., Ambrizzi, T. Regimes de Precipitação na América do Sul: Uma Revisão Bibliográfica. Revista Brasileira de Meteorologia, 25, 2, 185-204, 2010. https://doi.org/10.1590/S0102-77862010000200004.

[7] Brito, T.T., Oliveira-Júnior, J.F., Lyra, G.B., Gois, G., Zeri, M. Multivariate analysis applied to monthly rainfall over Rio de Janeiro state, Brazil. Meteorology and Atmospheric Physics, 129, 2, 469-478, 2016. https://doi.org/10.1007/s00703-016-0481-x.

[8] Dereczynski, C.P., Oliveira, J.S., Machado, C.O. Climatologia da Precipitação no Município do Rio de Janeiro. Revista Brasileira de Meteorologia, 24, 1, 24-38, 2009. https://doi.org/10.1590/S0102-77862009000100003.

[9] André, R.G.B., Marques, V.S., Pinheiro, F.M.A., Ferraudo, A.S. Identificação de regiões pluviometricamente homogêneas no estado do Rio de Janeiro, utilizando-se valores mensais. Revista Brasileira de Meteorologia, 23, 501-509, 2008. https://doi.org/10.1590/S0102-77862008000400009.

[10] Satyamurty, P., Mattos, L.F., Nobre, C.A., Silva Dias, P.L. Tropics - South America. In: Meteorology of the Southern Hemisphere. Ed. Kauly, D. J. and Vincent, D. G., Meteorological Monograph. American Meteorological Society, Boston, 119-139, 1998.

[11] Cataldi, M., Assad, L.P.F., Torres Júnior, A.R, Alves, J.L.D. Estudo da influência das anomalias da TSM do Atlântico Sul extratropical na região da Confluência Brasil-Malvinas no regime hidrometeorológico de verão do Sul e Sudeste do Brasil. Revista Brasileira de Meteorologia, 25, 513-524, 2010. https://doi.org/10.1590/S0102-77862010000400010.

[12] Lima, A.O., Lyra, G.B., Moraes, M., Oliveira-Júnior, J.F., Zeri, M., Cunha-Zeri, G. Extreme rainfall events over Rio de Janeiro State, Brazil: characterization using probability distribution functions and clustering analysis. Atmospheric Research, 247,

1-105221, 2021. https://doi.org/10.1016/j.atmosres.2020.105221.

[13] Cruz, E., Carvalho, D.F., Ceddia, M.B., Antunes, M.A.H., Aquino, R.M. Ocorrência de Veranicos no Estado do Rio de Janeiro. Revista de Engenharia Agrícola de Jaboticabal, 24, 1, 68-79, 2004. https://doi.org/10.1590/S0100-69162004000100009.

[14] Moraes, N.O., Pimentel, L.C.G., Marton, E. Simulações Numéricas da Formação de Ilha de Calor na Região Metropolitana do Rio de Janeiro. Anuário do Instituto de Geociências (Rio de Janeiro), 28, 2, 116-138, 2005. https://doi.org/10.11137/2005_2_116-138.

[15] Zeri, M., Oliveira-Júnior, J.F., Lyra, G.B. Spatiotemporal analysis of particulate matter, sulfur dioxide and carbon monoxide concentrations over the city of Rio de Janeiro, Brazil. Meteorology and Atmospheric Physics, 113: 139-152, 2011. https://doi.org/10.1007/s00703-011-0153-9.

[16] Oliveira-Júnior, J.F., Gois, G, Terassi, P.M.B., Silva Junior, C.A., Blanco, C.J.C., Sobral, B.S., Gasparini, K.A.C. Drought severity based on the SPI index and its relation to the ENSO and PDO climatic variability modes in the regions North and Northwest of the State of Rio de Janeiro - Brazil. Atmospheric Research, 212, 91-105, 2018. https://doi.org/10.1016/j.atmosres.2018.04.022.

[17] Serra, A.B., Ratisbonna, L. Clima do Rio de Janeiro. Ministério da Agricultura. Serviço de meteorologia, 2ª edição. Boletim Geográfico, Fundação Instituto Brasileiro de Geografia (IBGE), nº 214, p. 135, 1957.

[18] Strang, D. Considerações sobre as chuvas de janeiro de 1962 no Estado da Guanabara. Escritório de Meteorologia, 16p, 1962.

[19] Serra, A. B. Clima da Guanabara. Boletim Geográfico, Fundação Instituto Brasileiro de Geografia (IBGE), nº 214, p. 35, 1970.

[20] Machado, R.L., Ceddia, M.B., Carvalho, D.F., Cruz, E. S., Francelino, M.R. Spatial variability of maximum annual daily rain under different return periods at the Rio de Janeiro state, Brazil. Bragantia, 69, suppl., 77-84, 2010. https://doi.org/10.1590/S0006-87052010000500009.

[21] IBGE-Instituto Brasileiro de Geografia e Estatística. IBGE, Diretoria de Pesquisas, Coordenação de Trabalho e Rendimento, Pesquisa Nacional por Amostra de Domicílios Contínua 2014. Available in: < http://www.ibge.gov.br/estadosat/perfil.php?sigla=rj>. Accessed in 20 jul. 2015.

[22] Costa, C.D. Variabilidade Intranual da Precipitação Pluvial Mensal no Estado do Rio de Janeiro. Monografia (Graduação em Engenharia Florestal). Curso de Engenharia de Florestal, Universidade Federal Rural do Rio de Janeiro, Seropédica, RJ, 42p., 2010.

[23] R Development Core Team. R: A language and environment for statistical computing. R Foundation for Statistical Computing, Vienna, Austria. ISBN 3-900051-07-0, URL http://www.R-project.org. 2005.

[24] Schlotzhaver, S.D., Littell R.C. SAS System for elementary statistical analysis. 2ª ed. Cary, NC: SAS Institute Inc., p.456, 1999.

[25] Bartlett, M.S. Properties of sufficiency and statistical tests. Processings of the Royal Society, Series A, 160: 268–282, 1937. jstor.org/stable/96803.

[26] Snedecor, G., Cochran, W., William, G. Statistical Methods (8th Ed.). Ames, Iowa: Blackwell Publishing Professional. ISBN 978-0-8138-1561-9, 1989. Retrieved 2011-08-05.

[27] Box, G.E.P., Cox D. R. An analysis of processings. Journal of the Royal Statistical Society, Series B, 26: 211-252, 1964.

[28] Shapiro, S.S., Wilk, M.B. An Analysis of Variance Test for Normality (Complete Samples). Biometrika, 52, 1, 591-611, 1965.

[29] Ward, J.H. Hierarchical grouping to optimize an objective function. Journal of the American Statistical Association, 58, 1, 236-244, 1963. https://doi.org/10.1080/01621459.1963.10500845.

[30] Everitt, B.S., Dunn, G. Applied multivariate analysis. London: Edward Arnold, 400p, 1991.

[31] Lyra, G.B., Oliveira-Júnior, J.F., Zeri, M. Cluster analysis applied to the spatial and temporal variability of monthly rainfall in Alagoas state, Northeast of Brazil. International Journal of Climatology, 34, 13, 3546-3558, 2014. https://doi.org/10.1002/joc.3926.

[32] Kubrusly, L.S. Um procedimento para calcular índices a partir de uma base de dados multivariados. Pesquisa Operacional, 21, 1, 107-117, 2001. https://doi.org/10.1590/S0101-74382001000100007.

[33] Atlas Eólico do Rio de Janeiro. Governo do Estado do Rio de Janeiro, Secretaria de Estado de Energia, da Indústria Naval e do Petróleo, 2002.

[34] Correia Filho, W.L.F., Souza, P.H.A., Oliveira-Júnior, J.F., Terassi, P.M.B., Gois, G., Silva Junior, C.A., Sobral, B.S., Rangel, R.H.O., Pimentel, L.C.G. Investigating the characteristics and predictability of measured wind speed data over Rio de Janeiro, Brazil. Pure And Applied Geophysics, 1, 1-23, 2021. https://doi.org/10.1007/s00024-021-02751-w.

[35] Lemos, C. F., Calbete, N. Sistemas Frontais que atuaram no litoral de 1987-1995. Climanalise Especial-Edição comemorativa de 10 anos. MCT/INPE/

CPTEC, 1996.

[36] Ferreira, N. J., Sanches, M., Silva Dias, M.A.F. Composição da Zona de Convergência do Atlântico Sul em Períodos de El Niño e La Niña. Revista Brasileira de Meteorologia, 19, 89-98, 2004.

[37] Mello, C.R., Viola, M.R, Curi, N., Silva, A.M. Distribuição Espacial da Precipitação e da Erosividade da Chuva Mensal e Anual no Estado do Espírito Santo. Revista Brasileira de Ciência do Solo, 36, 6, 1878-1891, 2012. https://doi.org/10.1590/S0100-06832012000600022.

[38] Yazici, B., Yolacan, S. A comparison of various tests of normality. Journal of Statistical Computation and Simulation, 77, 2, 175-183, 2007. https://doi.org/10.1080/10629360600678310.

[39] Romão, X., Delgado, R., Costa, A. An empirical power comparison of univariate goodness-of-fit of normality. Journal of Statistical Computation and Simulation, 80, 5, 545-591, 2010. https://doi.org/10.1080/00949650902740824.

[40] Torman, V.B.L., Coster, R., Riboldi, J. Normalidade de variáveis: métodos de verificação e comparação de alguns testes não-paramétricos por simulação. Revista Hospital das Clínicas Paraná, 32, 2, 227-234, 2012.

[41] Pereira, M.A.F., Kobiyama, M. Análise de variâncias pluviométricas na região da bacia hidrográfica do Cubatão do Sul (SC). Ambiência (Online), 9, 1, 95-111, 2013. https://doi.org/10.5777/ambiencia.2013.01.07.

BILINGUAL PUBLISHING CO.
Pioneer of Global Academics Since 1984

Journal of Atmospheric Science Research
https://ojs.bilpublishing.com/index.php/jasr

ARTICLE

Dual Anthropogenic Origin of Global Warming through GHGs and IR Radiation Emissions from Artificialized Soils

Romdhane Ben Slama*

ISSAT Gabes, University of Gabes, Tunisia

ARTICLE INFO

Article history
Received: 2 August 2021
Accepted: 9 September 2021
Published : 25 October 2021

Keywords:
Greenhouse gazes
Global warming
Infrared radiation emission
Artificilised soils

ABSTRACT

This paper contributes to explain the global warming instead of "giving up" and thinking about passively adapting to climate change or global warming. It makes more sense to tackle what creates the greenhouse effect and contributes to global warming. The greenhouse effect is not only due to GHGs emissions, but also to the excess IR radiation emitted during the day, by artificial surfaces, following the absorption of solar radiation. The phenomenon should be compared to that of radiative forcing well known by climatologists and which makes the link between atmospheric pollution and the density of heat fluxes stopped by the atmosphere inducing global warming. It becomes clear that type an equation here. The surplus CO2 and IR radiation emissions influence global warming, not to mention the direct part of the heat released by the combustion of fossil fuels and even renewable (wood fires, biogas, friction of wind turbine propellers with the air).

1. Introduction

The responsibility for human activities is unequivocal in greenhouse gas emissions and the artificialization of soils. These, mainly due to the construction of roads, pavements, buildings, etc., have serious consequences for the environment [1,2]:

- Decrease in areas constituting carbon sinks .
- Modification of the albedo and therefore the perception of incident solar radiation: the first is reduced and therefore the second is increased in far infrared radiation emissions from artificial surfaces.

Table 1. Coefficient of albedo according to the nature of the surface

Surface	Albedo
Fresh asphalt	0.04
Wom asphalt	0.12
Forest	0.15
Bare soil	0.17
Desrt sand	0.40
New concrete	0.55
Ocean ice	0.60
Fresh snow	0.80

The dual anthropogenic origin of climate change: emission of GHGs and infrared radiation from artificialized

*Corresponding Author:
Romdhane Ben Slama,
ISSAT Gabes, University of Gabes, Tunisia;
Email: Romdhaneb.slama@gmail.com

DOI: https://doi.org/10.30564/jasr.v4i4.3502

soils has an issue that must be well understood in order to limit the earth's greenhouse effect and therefore global warming. To do this, it is useful to make the analogy between the greenhouse effect in a solar collector and the terrestrial greenhouse effect.

2. Methodology for Caracterizing the Greenhouse Effect

2.1 Greenhouse Effect Used in a Solar Collector

For those experienced in the field of solar energy [2], the greenhouse effect has always been used to allow solar collectors (water or air) to heat well. Indeed the collector without glazing does not heat too much, it may be used for low temperatures. The glass sensor (single or double) allows higher temperatures to be reached. The secret lies in the selectivity of the glazing which allows solar radiation to pass, the spectrum of which ranges from ultra-violet to near infrared [0.25 - 2.5 µm], and on the other hand is opposed to infrared radiation. Far wavelength that exceeds [4.1 - 41 µm], emitted by the dark surface of the absorber.

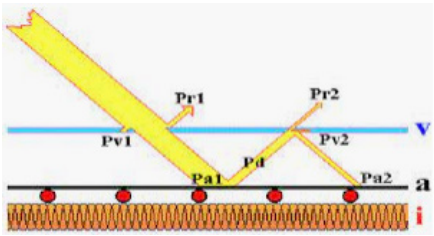

Figure 1. Construction of a double-glazed solar collector. Creation of the greenhouse effect.

Figure 2, the Black-body emission curves from the sun (T = 5780 K) and the earth (T= 290 K), shows the operation of Wien's Law. The two graphs are not to scale.

Indeed for the sun at 6000K, the corresponding average wavelength. λ_{mean} is given by:

$$\lambda_{mean} \frac{2898}{T} = 0.5\ \mu m$$

And the spectrum spreads to

$$0.5.\ \lambda_{mean} \text{ at } 5.\ \lambda_{mean}$$

$_T$hat is to say: [0.25 - 2.5 µm),

For the radiation emitted by the absorber assumed to be at 80 °C for example on average,

$$\lambda_{mean} = 8.2\ \mu m$$

And the spectrum spreads to 0.5. λ_{mean} to 5. $\lambda_{mean,}$ that is to say: [4.1 - 41 µm),

2.2 Terrestrial Greenhouse Effect

The terrestrial greenhouse effect is necessary for life on earth, however it is increased as a result of global anthropogenic emissions. These emissions concern not only GHGs but also infrared radiation emitted by artificial surfaces [4-14]. This contributes to global warming, further accentuated by the heat released by the combustion of fossil fuels, which moreover generate the greatest amount of greenhouse gases.

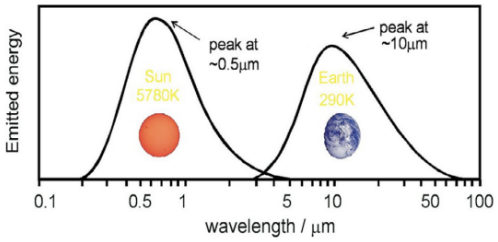

Figure 2. Solar and terrestrial radiative spectrum [3].

2.2.1 Greenhouse Gases

There are many greenhouse gases, more than forty have been identified by the Intergovernmental Panel on Climate Change (IPCC), including

- o water vapor (H_2O),
- o carbon dioxide (CO_2),
- o methane (CH_4),
- o ozone (O_3),
- o nitrous oxide (N_2O),
- o hydrofluorocarbons (HFCs),
- o perfluorocarbons (PFCs),
- o sulfur hexafluoride (SF6).

The proportions of anthropogenic greenhouse gases emitted by human activities are as Table 2 .

Table 2. Proportion and origin of GHGs

Gaz	Origin	Proportion
Carbon dioxyde (CO2)	• Combustion of fossil fuels (petroleum, coal), • Combustion of biomass.	70 %
Nitrous oxide (N2O)	• Agricultural activities, • Combustion of biomass and chemicals such as nitric acid.	14 %
Méthane (CH4)	• Agriculture (rice fields, livestock), • Production et distribution of gaz and oil, • Coal mining, • Combustion of petrolium and coal, • Landfills.	12 %
Fluorinated gazes (HFC, PFC, SF6)	• Refrigeration Systems, • Aerosols and insulating foams, • Semiconductors industry. Fluorating gases have a heating power 1,300 to 24,000 times that of carbon dioxide and have a very long service life. This is why they represent a real danger despite the modest share they represent in total GHG emissions	4 %

2.2.2 Contribution of Each Gas to the Greenhouse Effect

Different gases do not all contribute to the greenhouse effect at the same level. Indeed, some have a greater heating power than others and / or a longer lifespan. The contribution to the greenhouse effect of each gas is measured by the global warming potential (GWP).

The GWP is an indicator which groups together the added effects of the 6 gases contributing to the greenhouse effect which are currently taken into account by the Kyoto Protocol. It takes into account the radiative power returned by each gas to the ground (we speak of "radiative forcing"), accumulated over a period of 100 years.

This indicator is calculated using the respective GWP of the six gases considered. These GWPs are determined relative to that of CO_2, which is set at one [15].

Table 3. Global warming potential for GHGs

GHG	Relative GWP
Carbon dioxyde (CO2)	1
Methane (CH4)	21
Nitrous oxide (N2O)	310
Perfluorocarbons (PFC)	6 500 at 9 200 (depending on the molecules considered)
Hydrofluorocarbons (HFC)	140 at 11 700
Sulfur hexafluoride (SF6)	23 900

So,

• if we emit 1 kg of methane into the atmosphere, we will produce the same effect, over a century, as if we had emitted 21 kg of carbon dioxide;

• if we emit 1 kg of sulfur hexafluoride into the atmosphere, we will produce the same effect, over a century, as if we had emitted 23900 kg of carbon dioxide.

Not every gas contributes the same way to the GWP (global warming power or potential). In 2007, the contribution of GHGs to the PRG was established in metropolitan France as follows:

Table 4. Contribution of GHGs to the PRG

GHS	Contribution to GWP
Carbon dioxyde (CO2)	69.5 %
Méthane (CH4)	12.1 %
Nitrous oxide (N2O)	14.8 %
Fluorinated gases (HFC, PFC, SF6)	3.6 %

Source: CITEPA - Substances relatives à l'accroissement de l'effet de serre - Mai 2009.

In addition, greenhouse gas emissions are measured in carbon equivalent. The carbon equivalent of a gas is calculated from its GWP:

• by definition, 1 kg of CO_2 is equal to 0.2727 kg of carbon equivalent, ie the weight of carbon alone in the compound "carbon dioxide",

• for the other gases, the carbon equivalent is worth: relative GWP x 0.2727 (Table 5).

Table 5. Carbon equivalent of GHGs

GHGs	Carbon equivalent per kg emitted
Carbon dioxyde (CO_2)	0,273
Methane (CH_4)	5,73
Nitrous oxide (N_2O)	84,55
Perfluorocarbons (PFC)	1 772,73 à 2 372,73
Hydrofluorocarbons (HFC)	38,2 à 3 190,9
Sulfure Hexafluoride (SF_6)	6 518,2

Scientifically speaking, regarding global warming, we speak of the concept of radiative forcing, but commonly in public language of the greenhouse effect, which is half incorrect, because, during the day, an agricultural greenhouse heats up too much in the spring due to radiative forcing. In order to lower the temperature, it suffices to create a current of air when opening the doors.

The concentration of carbon dioxide affects the energy supply of the atmosphere; a first order approximation gives: The variation of the radiative forcing is:

DF = 5.35 {\displaystyle \Delta F=5.35\times \ln {C \over C_{0}}}

where C is the CO_2 concentration in parts per million by volume, ppm (v) or ppmv, and CO a reference concentration, for example, 280 ppm (v) for the CO_2 concentration at the threshold of the industrial age. ΔF is the change in radiative forcing in watts per square meter (Figure 3).

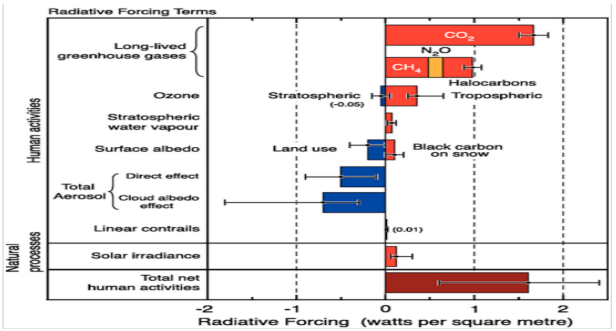

Figure 3. Radiative forcing of climate between 1750 and 2005 [16]

2.3 The Artificialization of Soils

This concerns roads, cities (building, urban expansion, etc.). Due to the fact that these soils can no longer absorb and store carbon dioxide, can no longer absorb rainwater, these soils will see:

- their reduced albedo (reflection coefficient of incident

sunlight) because their dark calor

- their increased absorption of solar radiation

- their increased infrared radiation emissions (this radiation will be returned to the earth by the atmosphere, all the more polluted causing greenhouse phenomenon by radiative forcing, and inducing the global warming.

The "protective mantle" that is our atmosphere is fragile: its way of filtering the sun's rays and conserving the earth's heat totally depends on the gases therein. For millions of years, it was essentially made of air (a mixture of nitrogen, oxygen, etc.). But, by adding more and more molecules, human beings have changed this balance enormously over the past sixty years.

Among these molecules, those called "greenhouse gases" are those which tend to heat the surface of the Earth by modifying its atmosphere. Greenhouse gases are molecules that absorb some of the infrared that the Earth's surface emits [17]. They thus prevent this heat from returning to space, as in a greenhouse which lets in the heat of the sun, but keeps it behind its windows. The main greenhouse gases are water vapor (H_2O), carbon dioxide (CO_2), methane (CH_4), nitrous oxide (N_2O), ozone (O_3) and several gases containing fluorine (such as CFCs and sulfur hexafluoride SF_6). By disturbing our atmosphere, these gases therefore cause overheating of the air and the surface of the Earth, but also a whole procession of disturbances of the movements of air in the atmosphere. This is called climate change. And it is high time to go back: for now, the enormous amounts of greenhouse gases that humans send into the atmosphere are partly "absorbed" by the oceans, but they are on the verge of indigestion.

3. Results and Discussion by Recapitulating

Table 6 recapitulates the effects of the actions of the man on the global warming and this by: 1) the gas emissions for purpose of greenhouse, but also by 2) the atificialision of the grounds which modify their albedo and thus the absorption of the solar radiation and thus their reheating and consequently their infrared emissions which is a fondamental component with the GHGs to cause the global warming. Finally one shows modification 3) due to heat released by the combustion of any type of combustible fossil or renewable [18]. Is it also allowed (finally?) to evoke the absorptive heat of the solar radiation by all the artificialized surfaces and become darker that what they were naturally.

4. Conclusions

The global warming du to the greenhouse effect ca be reduced by reducing the two factors that make it up according to the scientific name: radiative imprisonnement:

- For the factor: imprisonnement, there is a need to reduce the greenhouse gas emissions; and thus is known and evoked by all,

Table 6. Recapitulate

Naturally	**One century ago**	Clean atmospher → Terrestrial infrared radiation at 15 ° C → Desired greenhouse effect for the life on the earth
Humann Modification1	**Effet of combustion product CO2**	Clean atmospher; GHGs 35.10^9 tCO2e → Infrared Radiation at 15 °C → Imbalance. Increase of the Green House Effect → Global warming 2 to
Humann Modification2	**Effect of the artificialisation of the floors**	Clean atmosphere; Infrared Radiation at 15 °C; Radiation from artificialized floors → Imbalance. Increase of the Green House Effect → Global Warming ? at ? °C/centu

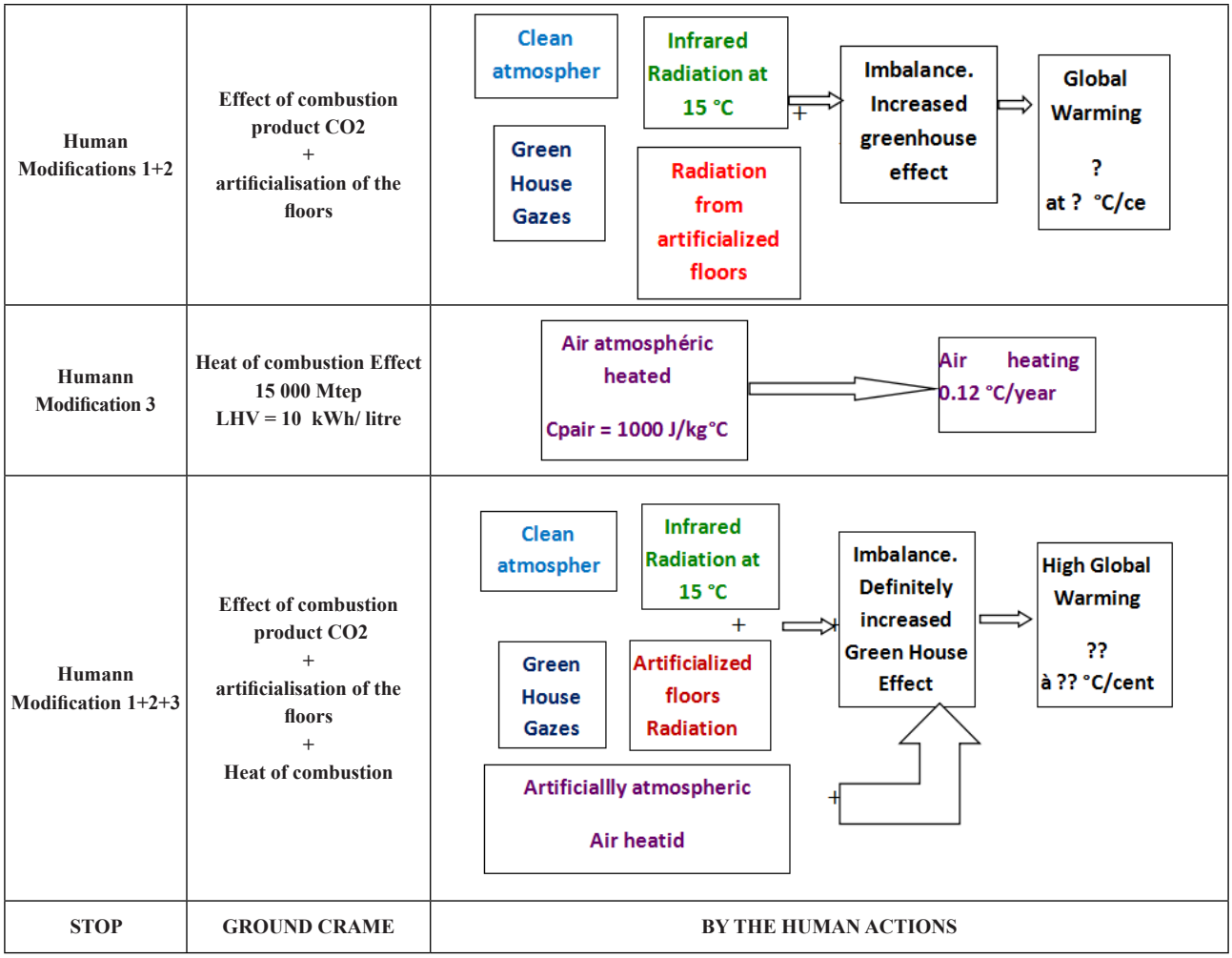

- For the factor: radiative, there is a need to reduce or at least limit the expansion of soil artificialisation which mainly concerns cities and roads, which absorb a lot of solar radiation during the day mainly because of their dark color , unlike bare soils.

References

[1] Knox RS (1999) Physical aspects of the greenhouse effect and global warming. American Journal of Physics 67: 1227.

[2] Kounkou (2012) Méthodologie pour la quantification de l'impact d'aménagements urbains sur un climat urbain modifie. Climatologie, numéro spécial 'Climats et changement climatique dans les villes'. https://doi.org/10.4267/climatologie.551.

[3] Ben Slama R. (2007) Apports solaires dans le bâtiment en Tunisie – Approche bioclimatique. 10éme Colloque de l'Association Internationale de Climatologie AIC 20: 99-104.

[4] https://www.researchgate.net/publication/325914607_Greenhouse_Gases.

DOI: 10.1016/B978-0-12-409547-2.14031-4.

[5] Ben Slama R. (2016) Green House Effect vs. Infrared Radiation Emissions. Journal of Climatology & Weather Forecasting 4: 1.

[6] Ben Slama R. (2017) Effet de serre vs émissions terrestres de rayonnement infrarouge: l'effet de serre n'est pas du qu'au dégagement des Gaz à Effet de Serre. Colloque 604. Congres de l'ACFAS 85éme édition, sur le thème :« Regards croisés sur l'adaptation aux changements climatiques dans le transport terrestre: Quelles formes, insuffisances et nouvelles pistes? Université McGill, Montréal, Quebec Canada.

[7] Ben Slama R. (2017) Role of the dark surfaces of cities on the greenhouse effect increase. Int.Conf.on Sustainible development» Ottawa, Ontario Canada, 9-10 August 2017. Visioconference.

[8] Ben Slama R. (2017) Effet de serre vs émissions terrestres de rayonnement infrarouge. L'effet de serre n'est pas dû qu'au dégagement des Gaz à effet de serre. Eau-Société-Climat'2017 (ESC-2017) Impacts Anthropiques et Climatiques sur la Variabilité des Ressources en Eau. Hammamet.

[9] Ben Slama R. (2017). L'Effet de serre et les radiations infrarouges des zones urbaines et goudronnées sombres. International Congress on Energetic and Environmental Systems (IEES-2017).

[10] Ben Slama R. Effet de serre vs émissions terrestres de rayonnement infrarouge : L'effet de serre n'est pas dû qu'au dégagement des Gaz à effet de serre. University of Gabes: Tunisia. 2017.

[11] Ben Slama R. Impact of the Artificial Surfaces Sunk on the Global Warming by the Absorption of the Solar Radiation and the Albedo Coefficient Modification. *J Climatol Weather Forecasting*. 2018;6:2.

[12] BEN SLAMA R., (2020) Global Warming and Its Multiple Causes. Journal of Atmospheric Science Research | Volume 03 | Issue 02 Pp 38-31.

[13] BEN SLAMA R (2021) Le réchauffement climatique accentué par les surfaces artificialisées qui absorbent le rayonnement solaire , émettent dans l'infrarouge et modifient l'albédo.. 88ème Congres de l'ACFAS 85éme édition, sur le thème :« Les changements climatiques et l'insécurité alimentaire : défis des pays développés et de ceux en voie de développement ? Université McGill, Montréal, Quebec Canada.

[14] Kokkila SI, Bera PP, Francisco JS, Lee TJ (2012) A group increment scheme for infrared absorption intensities of greenhouse gases. Journal of Molecular Structure 1009: 89-95.

[15] CITEPA - Substances relatives à l'accroissement de l'effet de serre - Mai 2009.

[16] https://planeteviable.org/forcage-radiatif-albedo-gaz-a-effet-de-serre/.

[17] https://www.archi7.net/J34/index.php/question-reponse/125-pourquoi-les-temperatures-du-jour-et-de-la-nuit-ne-sont-pas-tres-differentes.

[18] Szargut JT (2003) Anthropogenic and natural exergy losses (exergy balance of the Earth's surface and atmosphere). Energy 28: 1047-1054.
DOI: 10.1016/S0360-5442(03)00089-6.

BILINGUAL PUBLISHING CO.
Pioneer of Global Academics Since 1984

Journal of Atmospheric Science Research
https://ojs.bilpublishing.com/index.php/jasr

ARTICLE

North Atlantic Oscillation and Rainfall Variability in Southeastern Nigeria: A Statistical Analysis of 30 Year Period

Okorie, Fidelis Chinazor

Department of Geography and Environmental Management, Imo State University Owerri, Nigeria

ARTICLE INFO

Article history
Received: 18 October 2021
Accepted: 25 October 2021
Published: 29 October 2021

Keywords:
NAO
Rainfall variability
Relationship
Statistical analysis
Southeastern Nigeria

ABSTRACT

This study analyzed rainfall variability in Southeast region of Nigeria using graphical models, as well as using statistical approach to investigate any significant relationship between the global North Atlantic Oscillation (NAO) Index and the regional rainfall variability in region. The study was conducted in three States of Southeastern Nigeria namely, Abia, Ebonyi and Imo States that lie between Latitudes 4^0 40' and 8^0 50'N and Longitudes 6^0 20' and 8^0 50'E. Data for the study included 30 years (1988 - 2017) archival time-series monthly rainfall values for the three study States, acquired from Nigerian Meteorological Agency (NIMET), offices in the states, and Standardized values of NAOI (North Atlantic Oscillation Index) for the same period, which were collected from a website, on the NOAA Data Center, USA. In the data analyses, the first method was adopted by using graphs to illustrate mean annual rainfall values for thirty years. Coefficient of variability was employed in evaluating the degree of variability of values from the mean rate. The second analysis was accomplished using correlation models to ascertain any relationship between NAOI and rainfall in Southeast Nigeria. The results showed a significant variability of rainfall in the region from January to December (mean monthly) within the study period. A negative correlation value of 0.7525 was obtained from the correlation analysis, showing that the global NAO index and rainfall variability deviate in the opposite direction. Coefficient of multiple determinations (CMD) subsequently showed value of 0.031%, being the variation in rainfall as influenced by the global teleconnectivity, and this means that the NAO index has zero or no influence on rainfall variability in Southeast region of Nigeria.

1. Introduction

In recent years, the incidence of unusual weather patterns as they affect wet and dry season regimes have been observed in West African sub-region, including Nigeria. Sometimes, heavier rainfall than usual may occur and the rain is prolonged and extends into the dry season [1].

*Corresponding Author:
Okorie, Fidelis Chinazor,
Department of Geography and Environmental Management, Imo State University Owerri, Nigeria;
Email: fidelisokorie@yahoo.co.uk

DOI: https://doi.org/10.30564/jasr.v4i4.3843

The variability of rainfall is equally a necessary consideration in the tropics where rainfall is more eccentric than in temperate and also more seasonal in its occurrence within a year. The less eccentric, the more reliable rainfall is. Rainfall can vary in amount from one year, season, or month to month and may also show a downward or upward trend over a given period. According to [2], in the sub-Saharan region of Africa, climate variability has manifested essentially as rainfall variability.

The climate of Nigeria is however, a typical example of the climate of the West African sub-region. The variability of rainfall, defined as the average deviation from the mean, is enormous, sometimes up to 40-80% and increases with decreasing annual rainfall totals [3].

[4,5] reported the variations in rainfall intensified for different climatic regions and individual locations in Nigeria in the last century. [6], noted that climate variation generally occurs at different scales including local, regional, national and global scale.

[7], in a study ascertain there is variability in the weather and climate system of Imo State due to the observed shifts in rainfall within the 30 year climatic period. [8], indicates that shifts in rainfall and temperature regimes as well as evaporation and humidity conditions of southeastern Nigeria have been observed over time and the fluctuations however, are the atmospheric driving force that is responsible for the climate variations over the region. Another study [8], established that there is a variability and change in the weather and climate systems of Anambra state and entire southeastern Nigeria.

Increase in precipitation and changes in extremes, including floods would result to increased erosion and deterioration of groundwater quality, which would exacerbate many forms of water pollution [9]. This is because more sediment, nutrients, dissolved organic matter, pathogens, heavy metals, pesticides and salts are likely to infiltrate many aquifers more rapidly [10]. According to [11], rainfall variability can also affect agricultural productivity by decreasing outputs, which would negatively affect socio-economic wellbeing of the people. Hence, agriculture in the southeast region of Nigeria is adversely impacted by increasing variations in terms of timing and amount of rainfall.

Ever since, a variety of studies, more especially numerical modeling have been employed to analyze, as well as predict Sahel rainfall [12,13]. Although, these efforts have documented climate variations in West Africa, in recent times there has been little or no analysis of the forcing of climate trends particularly, in southeast region of Nigeria. For instance, what climatic factors control the nature and characteristics of the rain that falls in southeast Nigeria?

However, in this study the interest in the North Atlantic Oscillation and regional rainfall variability in southeast Nigeria. The North Atlantic Oscillation (NAO) index is based on the surface sea-level pressure difference between the Subtropical (Azores) High and the Sub-polar Low. The positive phase of the NAO reflects below-normal heights and pressure across the high latitudes of the North Atlantic and above-normal heights and pressure over the central North Atlantic, the eastern United States and Western Europe. The negative phase reflects an opposite pattern of height and pressure anomalies over these regions. Both phases of the NAO are associated with basin-wide changes in the intensity and location of the North Atlantic jet stream and storm track, and in large-scale modulations of the normal patterns of zonal and meridional heat and moisture transport, which in turn results in changes in temperature and precipitation patterns often extending from eastern North America to western and central Europe [14].

Strong positive phases of the NAO tend to be associated with above-normal temperatures in the eastern United States and across northern Europe and below-normal temperatures in Greenland and oftentimes across southern Europe and the Middle East. They are also associated with above-normal precipitation over northern Europe and Scandinavia and below-normal precipitation over southern and central Europe [15]. Opposite patterns of temperature and precipitation anomalies are typically observed during strong negative phases of the NAO. During particularly prolonged periods dominated by one particular phase of the NAO, abnormal height and temperature patterns are also often seen extending well into central Russia and north-central Siberia. The NAO exhibits considerable inter-seasonal and inter-annual variability, and prolonged periods (several months) of both positive and negative phases of the pattern are common. Studies indicate that the ENSO, which strength can be measured through an index, namely, the Southern Oscillation Index (SOI) influences West African rainfall [1,13]. The Southern Oscillation Index (SOI) is a standardized index based on the observed sea level pressure differences between Tahiti and Darwin, Australia [16].

Similarly, this study therefore, precisely intends to assess the influence of the North Atlantic Oscillation (NAO) on rainfall variability in southeast region of Nigeria. That means, trying to find out if there is any significant correlation between NAO and Rainfall variability in the region as the case in other countries for instance [17], used correlation analysis to study Relationship between the North Atlantic Oscillation Index and October- December Rainfall Variability over Kenya.

2. Area of Study

The study was conducted in three States of Southeastern Nigeria namely, Abia, Ebonyi and Imo States that lie between Latitudes 4^0 40' and 8^0 50'N and Longitudes 6^0 20' and 8^0 50'E (see Figure 1). These states cover about 16335.5 Km^2 in area. The study area lies in the humid tropical climate with annual rainfall ranging from 1500 mm in the northern part to 2500 mm in the southern part [18]. The mean annual temperature ranges from 24 ^{0}C to 30 ^{0}C [19].

However, the rainfall pattern is bimodal having peaks in July and September of the year with a short dry spell in August popularly referred to as 'August Break' or 'Little Dry Season'. Generally, the area has 8 months (March-October) of rainy season and 4 months (November- February) of dry season. Relative humidity of the area varies with seasons and a function of the prevailing air mass [20]. High relative humidity ranges from 80 to 90% at 10.00 am local time during rainy seasons when the westerly winds are prevalent. On the other hand, relative humidity ranges from 60 to 80% at 10.00 am local time during the dry season when northeast trade (Harmattan) winds prevail. Fluctuations in relative humidity exist on daily basis. In addition, mean monthly evapo-transpiration ranges from 4.0 to 4.5 mm/day during the dry periods of the year while values ranging from 2.5 to 3.5 mm/day characterize the evapo-transpiration of the rainy season. The drainage system is mainly influenced by Imo River, Ebonyi River, Aba River and their tributeries, and these influence soils, microclimate and land use activities. Most of these rivers move southwards to join larger bodies of water (see Figure 2).

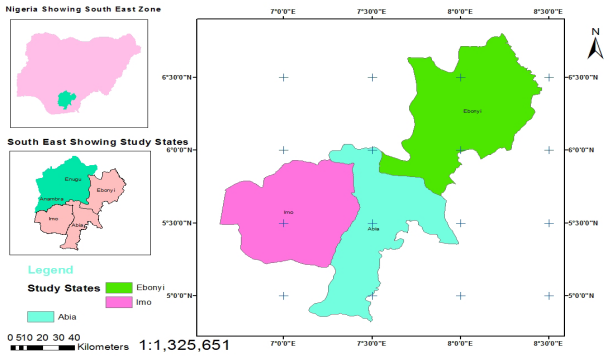

Figure 1. Location Map of the study area

Source: After Okorie 2021

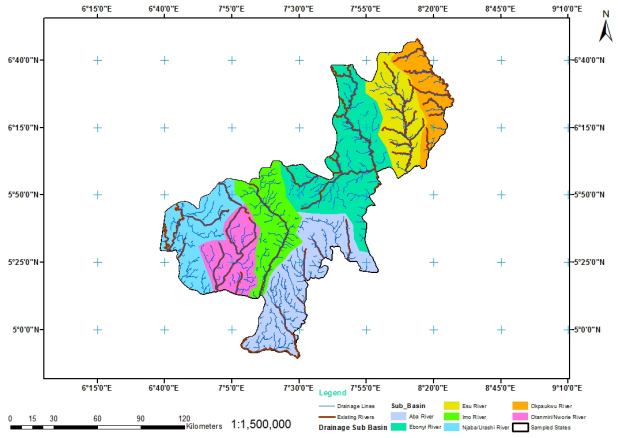

Figure 2. Drainage map of the study area showing the tributaries.

Source: Okorie, 2021.

3. Materials and Methods

The research activities comprised field studies for secondary data collection, and data analysis using statistical methods. The data therefore, included:

a. Archival time-series climatic data on monthly rainfall (in millimeters) for the three study states, acquired from Nigerian Meteorological Agency (NIMET), offices in the states.

b. Standardized values of NAOI (North Atlantic Oscillation Index), as complimentary data, which were collected from a website, on the climate database of NOAA, USA. Both the rainfall data and the NAOI values were for 30 years period, ranging from 1988 to 2017 (see Table 1 & Table 2).

The analysis for this study was approached in two main ways. First, rainfall variability patterns were analyzed and the second was the analysis linking Nigeria rainfall to the global North Atlantic Oscillation Index mode.

The first method was adopted by using line graphs modeling of annual values of rainfall, as well as their mean rate. Coefficient of variability was employed in evaluating the degree of variability of values from the mean rate. Meanwhile, the second analysis was accomplished using correlation models to ascertain any relationship between NAOI and rainfall in Southeast Nigeria.

4. Results and Discussions

Mean monthly rainfall in Southeastern Nigeria (1988-2017)

The results showed a significant variability of rainfall in the region from January to December (mean monthly) within the study period. December had the lowest with

Table 1. North Atlantic Oscillation (NAO) Index Values 1988 - 2017

S/N	Year	Jan	Feb	Mar	Apr	May	Jun	Jul	Aug	Sep	Oct	Nov	Dec	TOT	Mean
1	1988	1.02	0.76	-0.17	-1.17	0.63	0.88	-0.35	0.04	-0.99	-1.08	-0.34	0.61	-0.16	0.013
2	1989	1.17	2.00	1.85	0.28	1.38	-0.27	0.97	0.01	2.05	-0.03	0.16	-1.15	8.42	0.702
3	1990	1.04	1.41	1.46	2.00	-1.53	-0.02	0.53	0.97	1.06	0.23	-0.24	0.22	7.13	0.594
4	1991	0.86	1.04	-0.20	0.29	0.08	-0.82	-0.49	1.23	0.48	-0.19	0.48	0.46	3.22	0.268
5	1992	-0.13	1.07	0.87	1.86	2.63	0.20	0.16	0.85	-0.44	-1.76	1.19	0.47	6.97	0.581
6	1993	1.60	0.50	0.67	0.97	-0.78	-0.59	-3.18	0.12	-0.57	-0.71	2.56	1.56	2.15	0.179
7	1994	1.04	0-46	1.26	1.14	-0.57	1.52	1.31	0.38	-1.32	-0.97	0.64	2.02	6.45	0.586
8	1995	0.93	1.14	1.25	-0.85	-1.49	0.13	-0.22	0.69	0.31	0.19	-1.38	-1.67	-0.97	-0.081
9	1996	-0.12	-0.07	-0.24	-0.17	-1.06	0.56	0.67	1.02	-0.86	-0.33	-0.56	-1.41	-2.57	-0.214
10	1997	-0.49	1.70	1.46	-1.02	-0.28	-1.47	0.34	0.83	0.61	-1.70	-0.90	-0.96	-1.88	-0.152
11	1998	0.39	-0.11	0.87	-0.68	-1.32	-2.72	-0.48	-0.02	-2.00	-0.29	-0.28	0.87	-5.77	-0.481
12	1999	0.77	0.29	0.23	-0.95	0.92	1.12	-0.90	0.39	0.36	0.20	0.65	1.61	4.69	0.391
13	2000	0.60	1.70	0.77	-0.03	1.58	-0.03	-1.03	-0.92	-0.21	0.92	-0.92	-0.58	1.85	0.154
14	2001	0.25	0.45	-1.26	0.00	-0.02	-0.20	-0.25	-0.07	-0.65	-0.24	0.63	-0.83	-2.19	-0.183
15	2002	0.44	1.10	0.69	1.18	-0.22	0.38	0.62	0.38	-0.70	-2.28	-0.18	-0.94	0.47	0.039
16	2003	0.16	0.62	0.32	-0.18	0.01	-0.07	0.13	-0.07	0.01	-1.26	0.86	0.64	1.17	0.098
17	2004	-0.29	-0.14	1.02	1.15	0.19	-0.89	1.13	-0.48	0.38	-1.10	0.73	1.21	2.91	0.243
18	2005	1.52	-0.06	-1.83	-0.30	-1.25	-0.05	-0.51	0.37	0.63	-0.98	-0.31	-0.44	-3.21	-0.268
19	2006	1.27	-0.51	-1.28	1.24	-1.14	0.84	0.90	-1.73	-1.62	-2.24	0.44	1.34	-2.49	-0.208
20	2007	0.22	-0.47	1.44	0.17	0.66	-1.31	-0.58	-0.14	0.72	0.45	0.58	0.34	2.08	0.173
21	2008	0.89	0.73	0.08	-1.07	-1.73	-1.39	-1.27	-1.16	1.02	-0.04	-0.32	-0.28	-4.54	-0.378
22	2009	-0.01	0.06	0.57	-0.20	1.68	-1.21	-2.15	-0.19	1.51	-1.03	-0.02	-1.93	-2.92	-0.243
23	2010	-1.11	-1.98	-0.88	-0.72	-1.49	-0.82	-0.42	-1.22	-0.79	-0.93	-1.62	-1.85	-13.83	-1.153
24	2011	-0.88	0.70	0.61	2.48	-0.06	-1.28	-1.51	-1.35	0.54	0.39	1.36	2.52	3.52	0.293
25	2012	1.17	0.42	1.27	0.47	-0.91	-2.53	-1.32	-0.98	-0.59	-2.06	-0.58	0.17	-5.47	-0.456
26	2013	0.35	-0.45	-1.61	0.69	0.57	0.52	0.67	0.97	0.24	-1.28	0.90	0.95	2.52	0.21
27	2014	0.29	1.34	0.80	0.31	-0.92	-0.97	0.18	-1.68	1.62	-1.27	0.68	1.86	2.24	0.187
28	2015	1.79	1.32	1.45	0.73	0.15	-0.07	-3.18	-0.76	-0.65	0.44	1.74	2.24	5.2	0.433
29	2016	0.12	1.58	0.73	0.38	-0.77	-0.43	-1.76	-1.65	0.61	0.41	-0.16	0.48	-0.46	-0.038
30	**2017**	0.48	1.00	0.74	1.73	-1.91	0.05	1.26	-1.10	-0.61	0.19	-0.00	0.88	2.71	0.226
	Total														

Source: Website of the National Climatic Data Center US

mean of 11.53 mm to highest in September with mean of 379.21 mm. Steady increase in rainfall was recorded in the months starting from January with mean of 14.18 mm, February with 34.01 mm, March with 88.03 mm, April 169.94 mm, May with 280.94 mm, June with 310.47 mm, July with 314.05 mm, August with 324.37mm and September (the highest) with 379.21 mm. Then, recession occurred in October with 265.68 mm and dropped significantly in November and December with mean of 56.11 mm and 11.53 mm, respectively. However, there was a decrease in mean monthly rainfall in the region following the downward rainfall trend line (see Figure 3).

Average Annual rainfall in Southeastern Nigeria (1988-2017)

Mean annual rainfall in the region showed a dramatic variability in the series. From the mean minimum (lowest) of 142.22 mm in the beginning of second decade, 1998 to the maximum (highest) of 235.13 mm in the middle of (last) third decade, 2012. Low mean annual rainfall in the series occurred in 2004 with 154.41 mm, 1993 with 159.49 mm, 2000 with 167.95 mm, 2010 with 168.18 mm, 2009 with 170.57 mm, 2001 with 171.92 mm, 2002 with 173.01 mm, 1994 with 175.34 mm, 1992 with 175.60 mm, 1988 with 177.38 mm, 1991 with 181.04 mm, 1989 with 181.16 mm, and 2005 and 2014 with 182.03mm and 185.99mm, respectively. High mean rainfall in the series as well occurred in 2006 with 224.50 mm, 2013 with 312.34 mm, 2003 with 208.47 mm, 2015 with 206.75 mm, 1996 with 206.55 mm, 1997 with 206.01, 1995 with 201.95 mm, 2008 with 196.83 mm, 1990 with 196.74 mm, 2011 with 193.97 mm, 2007 with 189.24 mm, 1999 with 186.73 mm and 2017 with 186.55 mm. However, the rainfall variability showed upward trend throughout the study period, which means there was generally increased rainfall in the region from 1988 to 2017 as shown in Figure 3.

Table 2. Values of the mean Rainfall (in mm) for the States in 30 years

S/N	Year	Abia	Ebonyi	Imo	Mean
1	1988	196.8	121.8	213.6	177.38
2	1989	191.4	137.0	215.1	181.16
3	1990	169.8	173.6	246.8	196.74
4	1991	165.7	163.4	214.0	181.04
5	1992	182.6	142.2	202.0	175.6
6	1993	165.1	131.5	181.9	159.49
7	1994	185.9	121.3	218.8	175.34
8	1995	206.7	180.7	218.5	201.95
9	1996	234.2	160.0	225.5	206.55
10	1997	188.5	188.5	241.0	206.01
11	1998	165.2	124.8	136.7	142.22
12	1999	224.9	125.7	209.6	186.73
13	2000	140.9	168.2	194.8	167.95
14	2001	184.0	139.8	192.0	171.92
15	2002	204.4	143.5	171.1	173.01
16	2003	186.8	240.1	198.5	208.47
17	2004	159.3	157.0	146.9	154.41
18	2005	171.0	188.7	186.4	182.03
19	2006	169.9	236.2	267.4	224.5
20	2007	201.7	169.2	196.8	189.24
21	2008	199.7	184.9	205.9	196.83
22	2009	169.2	168.1	174.4	170.57
23	2010	192.3	136.0	176.2	168.18
24	2011	181.5	199.3	201.1	193.97
25	2012	174.3	294.9	236.2	235.13
26	2013	181.4	294.0	164.6	213.34
27	2014	178.5	210.8	168.7	185.99
28	2015	173.5	235.2	211.6	206.75
29	2016	171.2	254.8	180.6	202.19
30	2017	151.3	236.6	171.7	186.55
TOTAL		**5467.7**	**5427.8**	**5968.4**	**5621.24**

Source of data: NIMET, 2018

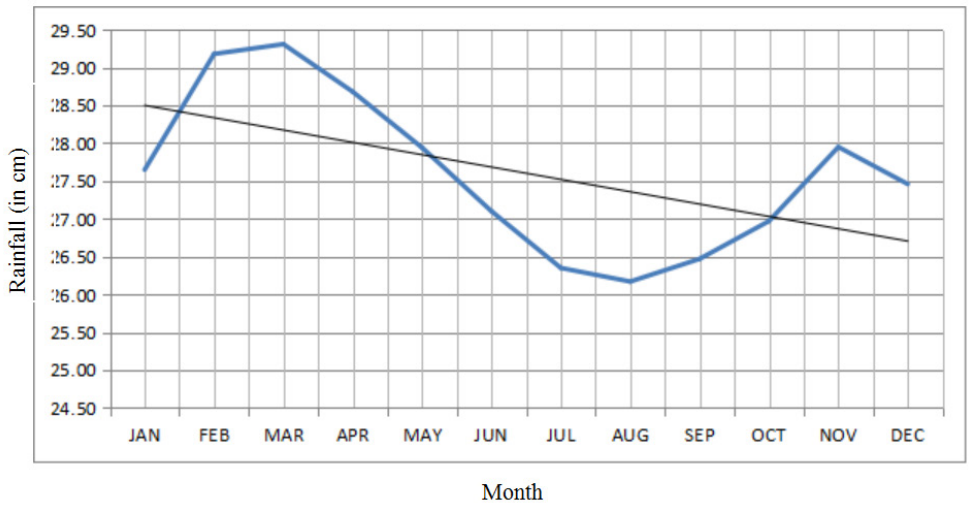

Figure 3. Mean monthly rainfall (in cm) for Southeastern Nigeria

Table 3. Values for Correlation of Rainfall with North Atlantic Oscillation Index

S/N	Year	NAO (X)	RF (Y)	NAO2 (X2)	RF2 (Y2)	NAO x RF (XY)
1	1988	0.013	177.38	0.000167	31463.66	2.30594
2	1989	0.702	181.16	0.4928	32818.95	127.17432
3	1990	0.594	196.74	0.3528	38706.63	116.86356
4	1991	0.268	181.04	0.0718	32775.48	48.51872
5	1992	0.581	175.6	0.3376	30835.36	102.0236
6	1993	0.179	159.49	0.0320	25437.06	28.54871
7	1994	0.586	175.34	0.3434	30744.12	102.74924
8	1995	-0.081	201.95	0.00656	40783.80	-16.35795
9	1996	-0.214	206.55	0.0458	42662.90	-44.2017
10	1997	-0.152	206.01	0.0231	42440.12	-31.31352
11	1998	-0.481	142.22	0.2314	20226.53	-68.40782
12	1999	0.391	186.73	0.1529	34868.09	73.01143
13	2000	0.154	167.95	0.0237	28207.20	25.8643
14	2001	-0.183	171.92	0.0335	29556.49	-31.46136
15	2002	0.039	173.01	0.0015	29932.46	6.74739
16	2003	0.098	208.47	0.0096	43459.74	20.43006
17	2004	0.243	154.41	0.0590	23842.45	37.52163
18	2005	-0.268	182.03	0.0718	33134.92	-48.78404
19	2006	-0.208	224.5	0.0433	50400.25	-46.696
20	2007	0.173	189.24	0.0230	35811.78	32.73852
21	2008	-0.378	196.83	0.1429	38742.05	-74.40174
22	2009	-0.243	170.57	0.0590	29094.12	-41.44851
23	2010	-1.153	168.18	1.3294	28284.51	-193.91154
24	2011	0.293	193.97	0.0858	37624.36	56.83321
25	2012	-0.456	235.13	0.2079	55286.12	-107.21928
26	2013	0.21	213.34	0.0441	45513.96	44.8014
27	2014	0.187	185.99	0.0350	34592.28	34.78013
28	2015	0.433	206.75	0.1875	42745.56	89.52275
29	2016	-0.038	202.19	0.0144	40880.80	-7.68322
30	2017	0.226	186.55	0.0511	34800.90	42.1603
TOTAL		**1.515**	**5621.24**	**4.512827**	**1065672.65**	**280.70853**

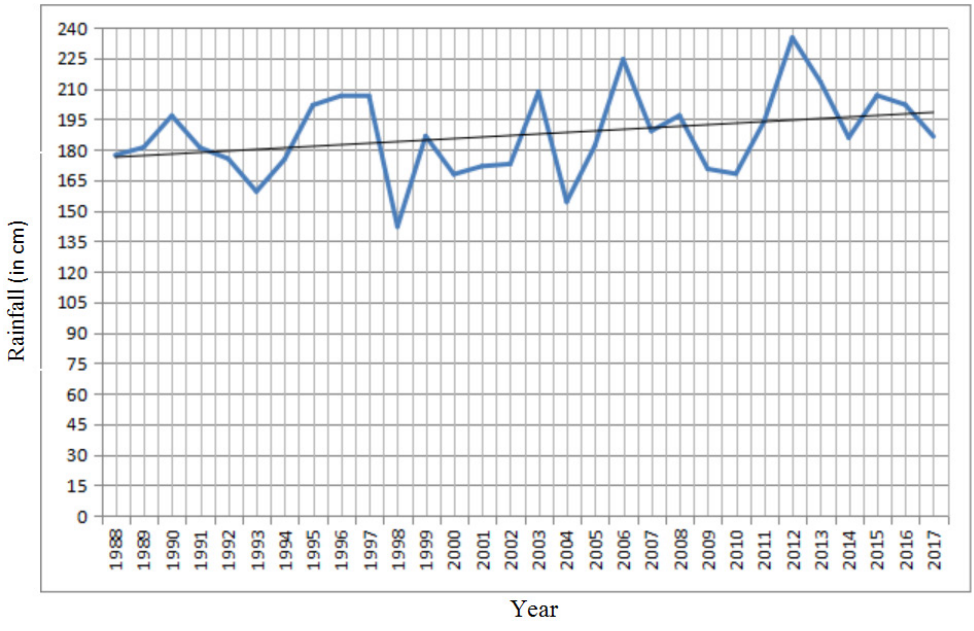

Figure 4. Mean Annual rainfall (in cm) for Southeast Nigeria

Relationship between NAO and Rainfall Variability

The correlation of Rainfall with NAOI is given as:

$$rNR\ (rxy) = \frac{n\sum NR - \sum N\sum R}{\sqrt{(n\sum N^2-(\sum N)^2)(n\sum R^2-(\sum R)^2)}} \text{ or } r = \frac{n\sum xy-\sum x\sum y}{\sqrt{(n\sum x-(\sum x)^2)\,x\,(n\sum y^2-(\sum y)^2)}}$$

Where, n = 30 (number of years)

R = Rainfall values (mm) = Y = dependent variable

N = NAO index values = X = independent variable

i.e.

n =30,

$\sum x = 1.515$,

$\sum y = 5621.24$,

$\sum x^2 = 4.51$,

$\sum y^2 = 1065672.65$, and

$\sum xy = 280.71$

Therefore, r =

$$\frac{30x280.71 - 1.52 \times 5621.24}{\sqrt{(30 \times 4.51 - 1.52^2)\,x\,(30 \times 1065672.65 - 5621.24^2)}} = \frac{-122.99}{\sqrt{7032.13}}$$

r = -0.0175

The correlation value of 0.7525 is a negative one, showing that the two variables (x and y) deviate in the opposite direction i.e., the increase in the values of x (variable) results, on an average, in a corresponding decrease in the values of y (variable), and the decrease in the values of x (variable) results, on an average, in a corresponding increase in the values of y (variable).

Coefficient of Multiple Determinants (CMD)

CMD is given as $100r^2$ (i.e., 100 x -0.0175^2) = 0.031%

This shows that about 0.031% of the changes or variations in y (variable) can be attributed to the influences of x (variable).

Test for significance with Student's T-Test model

To test for the significance level of the influences of x on y, we employ the student's t-test model. This is given a;

$$tc = \frac{r\sqrt{n-2}}{1-r^2}$$

Where;

tc is the calculated table (t-value), n-2 is the degree of freedom (DF), r is the correlation value of x against y, and n is 30 years (duration under investigation).

Therefore, $tc = \frac{0.0175\sqrt{30-2}}{1-0.0175^2} = 0.093$

At DF of 28, the probability for a t-value of 0.093 lies below 0.5 (i.e., 50%) This reveals a very low significance level of the influences x on y.

Since the coefficient of multiple determinations (CMD) is 0.031%, it shows that about 0.031% of the variation in rainfall can be attributed to North Atlantic Oscillation Index, which means that the NAO index has no influence on rainfall variability in Southeast region of Nigeria.

5. Conclusions

This study indicates that southeast region of Nigeria has over time been experiencing high rainfall variability. The results generally, indicate that rainfall variability showed upward trend throughout the study period, which means increased rainfall in the region from 1988 to 2017. This study is in consonance with results of some studies such as [21], which stated that in Nigeria generally; there is high variability of rainfall characterized by pronounced variability from year to year and place to place. The work also reported that onset of effective rainy season seems to have been delayed in an unpredictable manner in recent years without delay in cessation. Other studies by [22,12,23] indicated that rainfall in Nigeria is showing some discrepancies and swings, and these studies report that the late onset of rains has been showing persistent downward annual rainfall trends. From the statistical analysis, the study shows that there is no relationship between global NAO index and Nigerian rainfall. In other words, NAO does not have any influence or control on the rainfall variability in southeastern Nigeria.

References

[1] Nnaji A.O (2009): Implications of Current Climate Variation on Weather Conditions over Imo State, Journal of Biological and Environmental Sciences 2 22-23.

[2] Nnaji AO (2001): Forecasting Seasonal rainfall for agricultural decision-making in Northern Nigeria" Agricultural and ForestMeteorological 107: 193-205.

[3] Ayoade, J.O. (2004). Introduction to Climatology for the Tropics (2nd ed) Ibadan. Spectrum Books Limited.

[4] Nnaji, A. O, Njoku, J. D and Ume, C. U. (2006). "Environmental Controls of rainfall over northern Nigeria: identification and verification", *Environmental Research and Development Journal,* Faculty of Engineering and Environmental Sciences. Imo State University Owerri, Vol. 1 pp 86-93.

[5] Ogungbenro, S. B., & Morakinyo, T. E. (2014): Rainfall distribution and change detection across climatic zones in Nigeria. *Weather and Climate Extremes, 5-6*, 1-6.10.1016/j.wace.2014.10.002.

[6] Okorie, F. C., Okeke, I. C., Nnaji, A. O., Chibo, C. N and Pat-Mbano, E. C. (2012): Evidence of Climate Varaibility in Imo State of southeastern Nigeria. Proceedings of the 5th International Conference on Water, Climate and Environment, BALWOIS 2012- 28May

to 2 June 2012-Ohrid, Republic of Mecidonia, *Journal of Earth Science and Engineering, 2 (2012) 544-553. David Publisging Company, USA.*

[7] Okorie, F. C., Okeke, I. C., Nnaji, A. O., Chibo, C. N., Duru, P. N. (2011): Rainfall variability as evidence of Climate variation in Imo State of South-Eastern Nigeria. *International Journal of Sustainable Development Vol. 4 Number, 9 (2011.*

[8] Okorie, F. C., Pat N. Duru, and Ifeyinwna C. Okeke (2013): Analysis of climate variability in Anambra State of Nigeria using 30 years rainfall and temperature data. Proceedings of Davos Atmospheric and Cryosphere Assembly DACA-13 July 8-13 2013 Davos, Switzerland, *International Journal of Contemporary Studies Volume 1 No. 1 pp 232- 241.*

[9] Okorie, F. C. (2016): Precipitation Anomalies and its Effects in Port Harcourt Metropolis of Rivers State Nigeria. Proceedings of IUGG General Assembly, 22 June - 2 July 2015 Prague, Czech Republic, *International Journal of Scientific & Engineering Research* Volume 7, Issue 5, May 2016 Edition.

[10] Okeke, I. C. and Okorie, F. C. (2009): Rural Water Sources and Quality Implications in Ogburu and Ihiala Communities of Anambra State, in Igbozuruike, U. M. et al; Rural Water Supply in Nigeria. Imo State University Owerri Cape Publishers Owerri, 2010, pp. 121-129.

[11] Okorie, F. C (2020): Assessment of the Linkage between Rainfall variability and Arable Crop production in Enugu State Nigeria. Proceedings of African Climate Risks Conference (ACRC-2019) 7-9 October 2019. Addis Ababa, Ethiopia, *American Based Research Journal, Vol-9-Issue-4 April-2020 ISSN (2304-7151) Pp 11-22.*

[12] Nnaji, A.O (1999): Climate Variation in Sub-Saharan Region of Nigeria: A Study of Rainfall Variability in Northern Nigeria. Unpublished PhD thesis, University of Florida Gannesville.

[13] NOAA (2014): National Marine Fisheries Service. NOAA Current Fishery Statistics No. 2014.

[14] Balmaseda MA, Trenberth KE, Kallen E (2013) Distinctive climate signals in reanalysis of global ocean heat content. Geophys Res Lett 40: 1754-1759.

[15] Muhati FD, Ininda JM, Opijah FJ (2007) Relationship between ENSO parameters and the trends and periodic fluctuations in east African rainfall, J Kenya Meteorol Soc 1: 20-43.

[16] Liguori, G. & Di Lorenzo, E. Separating the North and South Pacific meridional modes contributions to ENSO and tropical decadal variability. *Geophys. Res. Lett.* 46, 906-915 (2019).

[17] Shilenje ZW, Ongoma V, Ogwang BA (2015) Relationship between the North Atlantic Oscillation Index and October- December Rainfall Variability Over Kenya, J Geol Geosci 4: 207.
DOI: 10.4172/2329-6755.1000207.

[18] Ogbodo, E. N. (2013). The fertility and mananegment imperatives of the degraded upland soils of Ebonyi state, Southeast, Nigeria. Niger. J. Soil Sci. 23 (2): 168-177.

[19] NIMET (Nigerian Meteorological Agency, Nigeria) (2008). Climate, Weather and Water Information, for Sustainable Development and Safety, NIMET, 2008, Abuja.

[20] Onweremadu, E. U. (2006). Application of Geographic Information System (GIS) on soils, land use and soil-related environmental problems in Southeastern Nigeria, PhD Thesis of the Department of Soil Science, University of Nigeria, Nsukka, Nigeria, 330pp.

[21] Okorie, F. C. (2021). Climatic and Edaphic Factors for Crop Production in Southeast Nigeria, Lambert Academic Publishing, August, 2021.

[22] Afiesimama, E. A, Pal, J., Abiodun, B. J, Gutowski, W. J and Adedoyin, A (2006). Simulation of West African monsoon using the Regcm3 Part I: Model validation and interannual variability, *Theor. Appl. Climolotol. 86: 23-37.*

[23] Odjugo, A. O., (2010): Regional evidence of climate change in Nigeria. Journal of Geography and Regional Planning Vol. 3(6), pp 142-150.

BILINGUAL
PUBLISHING CO.
Pioneer of Global Academics Since 1984

Tel:+65 65881289
E-mail: contact@bilpublishing.com
Website:ojs.bilpublishing.com

ISSN 2630-5119